Available online at www.sciencedirect.com
SCIENCE DIRECT®
Comput. Methods Appl. Mech. Engrg. 193 (2004) 953–987
Computer methods in applied mechanics and engineering
www.elsevier.com/locate/cma

Reproducing kernel element method Part II: Globally conforming I^m/C^n hierarchies

Shaofan Li [a,*], Hongsheng Lu [b], Weimin Han [c], Wing Kam Liu [b], Daniel C. Simkins [a]

[a] Department of Civil and Environmental Engineering, University of California, Berkeley, CA 94720, USA
[b] Department of Mechanical Engineering, Northwestern University, Evanston, IL 60208, USA
[c] Department of Mathematics, University of Iowa City, IA 52242, USA

Received 8 April 2003; received in revised form 15 July 2003; accepted 4 December 2003

Abstract

In this part of the work, a minimal degrees of freedom, arbitrary smooth, globally compatible, I^m/C^n interpolation hierarchy is constructed in the framework of reproducing kernel element method (RKEM) for arbitrary multiple dimensional domains. This is the first interpolation hierarchical structure that has been constructed with both minimal degrees of freedom and higher order smoothness or continuity over multi-dimensional domain. The proposed hierarchical structure possesses the generalized Kronecker property, i.e.

$$\partial^{\alpha}\Psi_I^{(\beta)}/\partial x^{\alpha}(x_J) = \delta_{IJ}\delta_{\alpha\beta}, \quad |\alpha|, |\beta| \leqslant m.$$

This contribution is the latest breakthrough of an outstanding problem—construction of a minimal degrees of freedom, globally conforming, I^m/C^n finite element interpolation fields on an arbitrary mesh or subdivision of multiple dimension.

The newly constructed globally conforming interpolant is a hybrid of a set of C^{∞} global partition polynomials with a highly smooth (C^n) compactly supported meshfree partition of unity. Examples of compatible RKEM hierarchical interpolations are illustrated, and they are used in a Galerkin procedure to solve differential equations.

Keywords: Approximation theory; Finite element method; Meshfree method; Reproducing kernel element method

1. Introduction

Since the invention of finite element methods (FEM) in 1950s, there have been demands in construction of smooth finite element (FE) shape functions over discretizations of an arbitrary domain of multiple dimensions. This is because in many engineering applications the related Galerkin weak formulations may

* Corresponding author. Tel.: +1-510-642-5362; fax: +1-510-643-8928.
E-mail address: li@ce.berkeley.edu (S. Li).

0045-7825/$ - see front matter
doi:10.1016/j.cma.2003.12.002

be involved with higher order derivatives of unknown functions. For instances to simulate static and dynamic behaviors of beams, plates, and shells structures, e.g. simulation of a DNA string, simulation of a thin film on a silicon substrate, or geometric modeling of a human torso. A Galerkin weak formulation with second order derivatives of the unknown displacement is required in these simulations. This has a few consequences: (1) it may be required to interpolate the first or the second derivatives of the unknown function on the boundary (which is denoted as I^1 or I^2 type interpolation); (2) it requires a globally $C^1(\Omega)$ conforming interpolation field.

Similar situations occur in computations of gradient elasticity and gradient plasticity problems as well, which are primary theoretical and computational models in nanoscale and microscale constitutive modelings in order to take into account of cohesive force or dislocation interactions. Furthermore, the classical force method of structural engineering is deeply rooted in complementary variational principle. To use stress functions based complementary variational weak formulations in FEM computations requires globally conforming $C^1(\Omega)$ interpolation field as well. It is because this very reason that force method based finite element methods have never thrived.

Note that in this paper the term, I^m *interpolation field*, denotes the interpolant that can interpolate the derivatives of an unknown function up to mth order, whereas the term C^n *interpolation field* denotes the interpolant having globally continuous derivatives up to its nth order derivative, and the term P^k *interpolation field* stands for the interpolant that can reproduce complete kth order polynomials.

Constructing a globally conforming I^m/C^n, $(n, m > 1)$ interpolation field in multiple dimension was *the challenge* in the early development of finite element methods. It attracted a group of very creative engineers and mathematicians working on the subject. Some of them were intellectual heavy weight of the time, e.g. Clough and Tocher [7], Bazeley et al. [3], Bogner et al. [6], de Veubeke [8,9], Argyris et al. [1], Irons [15], Felippa and Clough [10], Bramble and Zlámal [27], Birkhoff et al. [5], Birkhoff and Gordon [28], Birkhoff [29] and Barnhill et al. [2], among others.

However, the problem has never been solved in a satisfactory manner, as Hughes [14] commented in his critically acclaimed finite element textbook,

> Continuous (i.e. C^0) finite element interpolations are easily constructed. The same cannot be said for multi-dimensional C^1-interpolants. It has taken considerable ingenuity to develop compatible C^1-interpolation schemes for two-dimensional plate elements based on classical theory, and the resulting scheme have always been extremely complicated in one way or another.

During the past half century, it has been an outstanding problem to construct compatible higher order continuous finite element shape function in multiple dimensions. In general, it is difficult to construct a global compatible C^1 interpolation field in a multi-dimensional domain. Although there were a few compatible C^1 elements constructed in 2D case, e.g. Argyris element [1] or Bell's element [4], they usually require adding extra degrees of freedom on either nodal points or along the boundary or in the interior of the element to make it work (or eventually do not work well because of their complexity).

In fact, the problem is still one of open problems in computational geometry, needless to say the construction of an arbitrary continuous I^m/C^n interpolation field. In order to circumvent the difficulties in constructing higher order continuous interpolants, various mixed formulations have been developed over the years to relax the continuity requirement on finite element interpolation spaces. However, the problem does not entirely go away. To a large extent, it is translated into another problem—stability of mixed formulations. Most mixed weak formulations may not be coercive unless finite element interpolants used satisfy certain pre-requisites, e.g. Babuška–Brezzi condition. As it is well known, most lower order interpolation fields do not satisfy such condition.

As a matter of fact, in many engineering applications, the incompatible element is the only viable choice in numerical computations. During the past 50 years, a main theme of finite element method research is to

develop versatile finite element shape functions that are suitable for various mixed formulations. Nevertheless, no general solution has been found. Even though engineers invented the so-called patch test to examine applicability of various incompatible elements [16], serious-minded mathematicians privately view it as "*malpratice*" or "*variational crime*". Without exaggeration, this predicament in FEM has hinged the advancement of finite element technology.

Therefore, there have been keen interests in constructing higher order finite element interpolants, meshfree interpolants, or versatile partition of unities, which is a current research trend to improve state-of-the-art finite element technology and meshfree technology. Recent studies (e.g. Hao et al. [13], Liu et al. [20] Part I of this work) showed that by combining a meshfree interpolant with finite element interpolant one may generate a class of hybrid interpolation functions that may achieve higher order smoothness interpolation in multiple dimensions, which is unattainable by traditional finite element technique. This new technology is now termed as *reproducing kernel element method* (RKEM) (see Part I), which is in contrast to the early meshfree *reproducing kernel particle method* (RKPM) [12,17–19,21,22].

In this part of work, we present systematic procedures to construct I^m/C^n interpolants with minimal degrees of freedom in the framework of reproducing kernel element method. By combining so-called *global partition polynomials* with localized meshfree interpolants, we have developed a systematical procedure to successfully generate arbitrary continuous interpolation fields on any given finite element subdivision. We believed that this is the first successful solution to this half century old problem, in both computational mechanics and computational geometry, which has been elusive in the past.

The significance of this contribution is that one can build arbitrary smooth interpolation field on any arbitrary mesh discretization, so that it can be used in: (1) smooth surface fitting purely based on the data at nodal points; (2) Galerkin weak formulations that contain higher order derivatives, such as computations of plate and shell structures and in simulations of problems in gradient elasticity and gradient plasticity; (3) mixed formulations that require interpolation field satisfying Babuška–Brezzi condition, such as incompressible fluid flow and large deformation of nearly incompressible elastic materials.

2. Reproducing kernel element method

2.1. Global partition polynomial

Since we mainly concern of construction interpolants on multiple dimensions, it is convenient to use multi-index notation to express partial derivatives in multiple dimensions.

Let $\mathbf{Z}^d$ denote the set of all ordered d-tuples of non-negative integers. A multi-index is an ordered collection (d-tuple) of d nonnegative integers, $\alpha = (\alpha_1, \ldots, \alpha_d)$, and its length is defined as

$$|\alpha| = \sum_{i=1}^{d} \alpha_i. \tag{2.1}$$

We write $\alpha! = \alpha_1!\alpha_2! \cdots \alpha_d!$ and $\mathbf{x}^\alpha = x_1^{\alpha_1} x_2^{\alpha_2} \cdots x_d^{\alpha_d}$ $\forall \mathbf{x} \in \mathbb{R}^d$. For a differentiable function $f(\mathbf{x})$ and any α with $|\alpha| \leqslant k$,

$$D^\alpha f(\mathbf{x}) = \frac{\partial^{|\alpha|} f(\mathbf{x})}{\partial x_1^{\alpha_1} \cdots \partial x_d^{\alpha_d}} \tag{2.2}$$

is the αth order partial derivative. As usual, $D^0 f(\mathbf{x}) = f(\mathbf{x})$.

To review the concept of finite element interpolation, a few definitions are in order.

Definition 2.1 (*Polygon subdivision*). A partition $\mathscr{T}_{n_{\text{el}}} = \{\Omega_1, \Omega_2, \ldots, \Omega_{n_{\text{el}}}\}$ of Ω is called a polygon subdivision if

- Ω_i is a polygon ($i = 1, 2, \ldots, n_{\text{el}}$).
- $\Omega_i \cap \Omega_j = \emptyset$ ($i \neq j$).
- $\mathscr{T}_{n_{\text{el}}}$ is a finite open cover of Ω, i.e. $\bigcup_{i=1}^{n_{\text{el}}} \overline{\Omega}_i = \overline{\Omega}$.
- If $\overline{\Omega}_i \cap \overline{\Omega}_j$ ($i \neq j$) consists of exactly one point, then it is the common vertex of Ω_i and Ω_j.
- If $\overline{\Omega}_i \cap \overline{\Omega}_j$ ($i \neq j$) consists of more than one point, then $\overline{\Omega}_i \cap \overline{\Omega}_j$ is the common surface, or common edge between Ω_i and Ω_j.

where index n_{el} is the total number of elements.

Definition 2.2 (*Partition of unity*). Let $\Omega \subset \mathbb{R}^d$ ($d = 1, 2, 3$) be an open bounded domain. Let $\Omega_1, \Omega_2, \ldots, \Omega_{n_p}$ be a family of finite open set in $\mathbb{R}^d$, and

1. The family of an open set $\{\Omega_I\}_{I \in \Lambda_P}$, $\Lambda_P := \{1, 2, \ldots, n_p\}$, generates a finite covering for domain Ω,

$$\Omega \subset \bigcup_{I \in \Lambda_P} \Omega_I. \tag{2.3}$$

2. There exists a family of functions, $\Psi_I \in C_0^s(\mathbb{R}^d)$, $s \geqslant 0$, and $\text{supp}\{\Psi_I\} \subset \overline{\Omega}$.
3. $\{\Psi_I(\mathbf{x})\}$ are positive and finite, $0 \leqslant \Psi_I(\mathbf{x}) \leqslant 1$ $\forall \mathbf{x} \in \Omega_I$.
4. The summation

$$\Psi_1(\mathbf{x}) + \Psi_2(\mathbf{x}) + \cdots + \Psi_{n_p}(\mathbf{x}) = 1 \quad \forall \mathbf{x} \in \Omega. \tag{2.4}$$

The family of generating function, or the interpolation basis, $\{\Psi_I\}_{I \in \Lambda_P}$ is called a *partition of unity* subordinate to the finite open cover $\{\Omega_I\}_{I \in \Lambda_P}$.

For practical purposes, we only consider finite open covers. The last property (2.4) suggests the name of *partition of unity*. The other distinguished property of the partition of unity is that the set, $\{\Omega_I\}_{I \in \Lambda_P}$, can be overlapping, and they do not necessarily form a subdivision (mesh) of Ω.

Finite element shape functions, $\phi_{e,i}$, $e \in \Lambda_E := \{1, 2, \ldots, n_{\text{el}}\}$, and $i \in \Lambda_e = \{1, \ldots, n_{\text{ne}}\}$, are compactly supported, $\text{supp}\{\phi_{e,i}\} = \overline{\Omega}_e$, where n_{el} is the total number of elements, Λ_e is the local index set for all the nodal points in an element, and the total number nodal points in a typical element, e, is n_{ne}. When $\mathbf{x} \notin \Omega_e$, $\phi_{e,i}(\mathbf{x}) = 0$.

For a large class of FEM shape functions, this condition is enforced by multiplying Heaviside function with certain global polynomial functions, or more precisely,

$$\phi_{e,i}(x) = \psi_{e,i}(x)\chi_e(x), \tag{2.5}$$

where function, $\chi_e(x)$, is the characteristic function of element e, i.e.

$$\chi_e(x) := \begin{cases} 1, & x \in \Omega_e, \\ 0, & x \notin \Omega_e. \end{cases} \tag{2.6}$$

The characteristic function in (2.6) truncates the analytical polynomial functions such that FEM shape functions are localized in compact supports. Because of the presence of the characteristic function, $\chi_e(x)$, most of FEM shape functions, $\phi_{e,i}(x)$, are $C^0(\Omega)$ functions in multiple dimensions.

We name the set of polynomial functions, $\psi_{e,i}(x)$ as *the global partition polynomials*. The so-called *global partition polynomial* may be viewed as the continuous extension of regular FEM polynomial shape func-

tion, [1] and it is defined in $\mathbb{R}^d$. Denote such globally continuous extension of a FEM shape functions, $\phi_{e,i}(\mathbf{x})$, as $\psi_{e,i}(\mathbf{x})$ where $e \in \Lambda_E$, and $i \in \Lambda_e$. Then a localized regular FEM shape function has one-to-one correspondence with a global partition polynomial, i.e.

$$\phi_{e,i} \in C^k(\Omega_e) \leftrightarrow \psi_{e,i} \in C^\infty(\mathbb{R}^d). \tag{2.7}$$

The global partition polynomials have two special properties. First, if a FEM shape function has the following Kronecker delta properties

$$D^\alpha \phi_{e,i}^{(\beta)}|_{\mathbf{x}=\mathbf{x}_j} = \delta_{ij}\delta_{\alpha\beta}, \quad \mathbf{x}_i, \mathbf{x}_j \in \overline{\Omega}_{e,i}, \ \ |\alpha|, |\beta| \leqslant m, \tag{2.8}$$

then the corresponding global polynomial function has the properties, i.e.

$$D^\alpha \psi_{e,i}^{(\beta)}|_{\mathbf{x}=\mathbf{x}_j} = \delta_{ij}\delta_{\alpha\beta}, \quad \mathbf{x}_i, \mathbf{x}_j \in \overline{\Omega}_{e,i}, \ \ |\alpha|, |\beta| \leqslant m. \tag{2.9}$$

In fact, in most cases, (2.8) is a consequence or built in property of (2.9).

Second, as a partition of unity under Λ_P, traditional finite element interpolants satisfy the condition,

$$\sum_{I \in \Lambda_P} \phi_I(\mathbf{x}) = 1 \quad \forall \mathbf{x} \in \overline{\Omega}. \tag{2.10}$$

However, since global partition polynomials are not compactly supported, they do not form a partition of unity for the global index set, Λ_P, i.e.

$$\sum_{I \in \Lambda_P} \psi_I(\mathbf{x}) \neq 1 \quad \forall \mathbf{x} \in \overline{\Omega}. \tag{2.11}$$

Nevertheless, the global partition polynomial has the following amiable properties: *the global partition polynomial forms a partition of unity in every local index set* Λ_e, i.e.

$$\sum_{i \in \Lambda_e} \psi_{e,i}(\mathbf{x}) = 1 \quad \forall \mathbf{x} \in \mathbb{R}^d \text{ and } \forall e \in \Lambda_E. \tag{2.12}$$

In general, if

$$\sum_{i \in \Lambda_e} \phi_{e,i}(\mathbf{x})\mathbf{x}_i^\beta = \mathbf{x}^\beta \quad \forall \mathbf{x} \in \Omega_e, \ \ e \in \Lambda_E \tag{2.13}$$

then one also has

$$\sum_{i \in \Lambda_e} \psi_{e,i}(\mathbf{x})\mathbf{x}_i^\beta = \mathbf{x}^\beta \quad \forall \mathbf{x} \in \mathbb{R}^d, \ \ e \in \Lambda_E. \tag{2.14}$$

The proof is self-evident, because

$$\sum_{i \in \Lambda_e} \phi_{e,i}(\mathbf{x})\mathbf{x}_i^\beta = \mathbf{x}^\beta \quad \forall \mathbf{x} \in \Omega_e \Rightarrow \sum_{i \in \Lambda_e} \psi_{e,i}(\mathbf{x})\mathbf{x}_i^\beta = \mathbf{x}^\beta \quad \forall \mathbf{x} \in \Omega_e. \tag{2.15}$$

On the other hand, $\{\psi_{e,i}(\mathbf{x})\}$ are $C^\infty(\mathbb{R}^d)$ elementary polynomials, and a finite linear combination of $\psi_{e,i}(\mathbf{x})$ will still be a $C^\infty(\mathbb{R}^d)$ elementary polynomial with the fixed order. Therefore,

$$\sum_{i \in \Lambda_e} \psi_{e,i}(\mathbf{x})\mathbf{x}_i^\beta = \mathbf{x}^\beta \quad \forall \mathbf{x} \in \Omega_e \Rightarrow \sum_{i \in \Lambda_e} \psi_{e,i}(\mathbf{x})\mathbf{x}_i^\beta = \mathbf{x}^\beta \quad \forall \mathbf{x} \in \mathbb{R}^d, \ \ e \in \Lambda_E. \tag{2.16}$$

[1] In this paper, we only consider polynomial type of FEM shape functions.

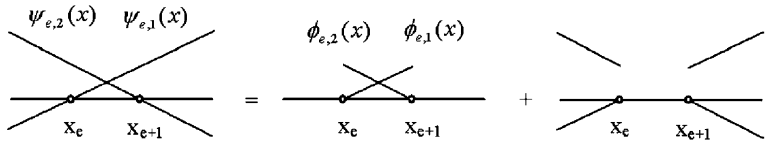

Fig. 1. Comparison of the global partition polynomial and FEM shape function.

Examples of one-dimensional (1D) partition polynomials are the following linear polynomials defined in $\mathbb{R}$,

$$\psi_{e,1}(x) = \frac{x_{e+1} - x}{x_{e+1} - x_e}, \tag{2.17}$$

$$\psi_{e,2}(x) = \frac{x - x_e}{x_{e+1} - x_e}, \tag{2.18}$$

where $-\infty < x < \infty$ and $e \in \Lambda_E$. In Fig. 1, the global partition polynomials defined in (2.17) and (2.18) are displayed, and they are compared with the 1D linear FEM shape function.

A two-dimensional example of global partition shape function set is:

$$\psi_{e,1}(\xi(\mathbf{x}), \eta(\mathbf{x})) = \tfrac{1}{4}(1 - \xi)(1 - \eta), \tag{2.19}$$

$$\psi_{e,2}(\xi(\mathbf{x}), \eta(\mathbf{x})) = \tfrac{1}{4}(1 + \xi)(1 - \eta), \tag{2.20}$$

$$\psi_{e,3}(\xi(\mathbf{x}), \eta(\mathbf{x})) = \tfrac{1}{4}(1 + \xi)(1 + \eta), \tag{2.21}$$

$$\psi_{e,4}(\xi(\mathbf{x}), \eta(\mathbf{x})) = \tfrac{1}{4}(1 - \xi)(1 + \eta) \tag{2.22}$$

with $-\infty < \xi, \eta < \infty$ and functions $\xi(\mathbf{x})$ and $\eta(\mathbf{x})$ can be found by its inverse relationship,

$$\mathbf{x} = \sum_{i=1}^{4} \psi_{e,i}(\boldsymbol{\xi}) \mathbf{x}_{e,i}. \tag{2.23}$$

2.2. RKEM interpolant

Now we describe how to construct a valid RKEM interpolant. In Part I of this work [20], the reproducing kernel element interpolation is expressed as

$$\mathscr{I} f(\mathbf{x}) = \sum_{e \in \Lambda_E} \left[\int_{\Omega_e} \mathscr{K}_\rho(\mathbf{x} - \mathbf{y}; \mathbf{x}) \, \mathrm{d}\mathbf{y} \left(\sum_{i \in \Lambda_e} \psi_{e,i}(\mathbf{x}) f(\mathbf{x}_{e,i}) \right) \right]. \tag{2.24}$$

To obtain a valid interpolation scheme, the integral in expression (2.24) is replaced by nodal integration,

$$\mathscr{I}^h f(\mathbf{x}) = \mathop{\mathbf{A}}_{e \in \Lambda_E} \left[\left(\sum_{j \in \Lambda_e} \mathscr{K}_\rho(\mathbf{x} - \mathbf{x}_{e,j}; \mathbf{x}) \Delta V_{e,j} \right) \left(\sum_{i \in \Lambda_e} \psi_{e,i}(\mathbf{x}) f(\mathbf{x}_{e,i}) \right) \right], \tag{2.25}$$

where $\Delta V_{e,j}$ is the nodal integration weight, which can be easily assigned for each meshfree particle depending on its residing position. The symbol, $\mathbf{A}_{e \in \Lambda_E}$, denotes the summation over all elements of the mesh.

The reproducing kernel function, $\mathscr{K}^{\varrho}_{e,j}(\mathbf{x}) := \mathscr{K}_{\varrho}(\mathbf{x}-\mathbf{x}_{e,j};\mathbf{x})$ is a compact supported function and the radius of its support, $\mathrm{supp}\{\mathscr{K}^{\varrho}_{e,j}(\mathbf{x})\}$, is $\varrho_{e,j}$. A smooth window function $C^n(\Omega)$ is chosen to serve as the core of the kernel.

Note that the RKEM nodal integration is consistent with the nodal integration employed in previous reproducing kernel particle method (RKPM) (e.g. in [23]) that ensures all the reproducing properties in discrete sense and guarantees that discrete summation is a partition of unity.

To ensure the global compatibility, the RKEM kernel function has to satisfy the following partition of unity conditions $\forall \mathbf{x} \in \Omega$

$$\mathop{\mathbf{A}}_{e\in\Lambda_E}\left\{\left(\sum_{j\in\Lambda_e}\frac{1}{\rho^d_{e,j}}w\left(\frac{\mathbf{x}-\mathbf{x}_{e,j}}{\rho_{e,j}}\right)b(\mathbf{x})\Delta V_{e,j}\right)\left(\sum_{i\in\Lambda_e}\psi_{e,i}(\mathbf{x})\right)\right\}=1. \tag{2.26}$$

One can then solve (2.26) to obtain the unknown $b(\mathbf{x})$,

$$b(\mathbf{x})=\left\{\mathop{\mathbf{A}}_{e\in\Lambda_E}\left[\left(\sum_{j\in\Lambda_e}\frac{1}{\rho^d_{e,j}}w\left(\frac{\mathbf{x}-\mathbf{x}_{e,j}}{\rho_{e,j}}\right)\Delta V_{e,j}\right)\left(\sum_{i\in\Lambda_e}\psi_{e,i}(\mathbf{x})\right)\right]\right\}^{-1}. \tag{2.27}$$

In FEM literature, the mapping

$$C_I:(e,i)\to I:\Lambda_E\times\Lambda_e\to\Lambda_P \tag{2.28}$$

between the local index pair (e,i) and global index I is called the connectivity. Assume the discretization mesh having the following surjective connectivity map $\Lambda_E\times\Lambda_e\to\Lambda_P$,

$$(e_1,i_1),(e_2,i_2),\ldots,(e_k,i_k),\ldots,(e_\ell,i_\ell)\to I. \tag{2.29}$$

The reproducing kernel element shape function can then be obtained

$$\Psi_I(\mathbf{x}):=\sum_{k=1}^{\ell}\left(\sum_{j\in\Lambda_{e_k}}\frac{1}{\rho^d_{e_k,j}}w\left(\frac{\mathbf{x}-\mathbf{x}_{e_k,j}}{\rho_{e_k,j}}\right)\Delta V_{e_k,j}\right)b(\mathbf{x})\psi_{e_k,i_k}(\mathbf{x}). \tag{2.30}$$

The reproducing kernel element interpolant can be expressed as

$$\mathscr{I}^h f(\mathbf{x})=\sum_{I\in\Lambda_P}\Psi_I(\mathbf{x})f_I. \tag{2.31}$$

An interpolation error estimate for the interpolation defined in (2.31) has been given in Part I of this work [20].

Proposition 2.1. *Consider the reproducing kernel element interpolant* (2.25). *Assume the discretization mesh having the following surjective connectivity map* $\Lambda_E\times\Lambda_e\to\Lambda_P$,

$$(e_1,i_1),(e_2,i_2),\ldots,(e_k,i_k),\ldots,(e_\ell,i_\ell)\to I. \tag{2.32}$$

Define

$$\Omega_I=\bigcup_{k=1}^{\ell}\Omega_{e_k}. \tag{2.33}$$

If $(e,i)\to I$, *the RKEM interpolant decomposition in an element may be denoted as*,

$$\mathscr{K}^{\rho}_{e,i}(\mathbf{x}):=\mathscr{K}_{\rho}(\mathbf{x}-\mathbf{x}_{e,i};\mathbf{x})=:\mathscr{K}^{\rho}_{I}(\mathbf{x})\quad\forall\mathbf{x}\in\Omega_e. \tag{2.34}$$

Suppose that

1. $$\sum_{i\in\Lambda_e}\psi_{e,i}(\mathbf{x})\mathbf{x}_i^{\lambda}=\mathbf{x}^{\lambda}\quad\forall\mathbf{x}\in\Omega,\ \ \lambda\leqslant\ell. \tag{2.35}$$
2. *Discretization mesh* $\mathscr{T}_{n_{\mathrm{el}}}$ *is quasi-uniform.*
3. *Meshfree interpolant is a signed partition of unity,*
$$\mathop{\mathbf{A}}_{e\in\Lambda_E}\left(\sum_{i\in\Lambda_e}\mathscr{K}^{\rho}_{e,i}(\mathbf{x})\right)=1\quad\forall\mathbf{x}\in\Omega. \tag{2.36}$$
4. *For* $e\in\Lambda_E$ *and* $(e,i)\to I$,
$$\mathrm{supp}\{\mathscr{K}^{\rho}_{e,i}(\mathbf{x})\}\subset\Omega_I. \tag{2.37}$$

The reproducing kernel element interpolation field

$$\mathscr{I}^h f=\sum_{I\in\Lambda_P}\Psi_I(\mathbf{x})f_I,$$

where

$$\Psi_I(\mathbf{x})=\sum_{k=1}^{\ell}\left(\sum_{j\in\Lambda_{e_k}}\mathscr{K}^{\rho}_{e_k,j}(\mathbf{x})\Delta V_{e_k,j}\right)\psi_{e_k,i_k}(\mathbf{x}),\quad I\in\Lambda_p \tag{2.38}$$

has the following properties,

1. $$\mathscr{I}^h\mathbf{x}^{\lambda}=\mathbf{x}^{\lambda},\quad\lambda=0,\ldots,k, \tag{2.39}$$
in particular $\mathscr{I}^h 1=1$,
2. $$\Psi_I(\mathbf{x}_J)=\delta_{IJ}. \tag{2.40}$$

The proof of the above statement is essentially the same as what have been given in the Part I of this series.

3. Globally conforming I^m/C^n hierarchy I

3.1. Construction

In this section, we construct the globally conforming I^m/C^n hierarchical interpolant family.

Consider the nodal point i of the element $e\in\Lambda_E$. Assume that one find a global partition polynomial basis, $\psi^{(0)}_{e,i}(\mathbf{x})$, such that

$$D^{\alpha}\psi^{(0)}_{e,i}\Big|_{\mathbf{x}=\mathbf{x}_j}=\delta_{\alpha 0}\delta_{ij},\quad|\alpha|\leqslant q. \tag{3.41}$$

We can then construct a hybrid meshfree/FEM interpolant basis as

$$\Psi^{(0)}_I(\mathbf{x})=\mathop{\mathbf{A}}_{e\in\Lambda_E}\left(\sum_{j\in\Lambda_e}\mathscr{K}^{\rho}_{e,j}(\mathbf{x})\Delta x_{e,j}\right)\psi^{(0)}_{e,i}(\mathbf{x}), \tag{3.42}$$

where connectivity $(e,i) \to I$ is implied. The meshfree kernel functions satisfy the following condition,

$$\mathop{\mathbf{A}}_{e\in\Lambda_E}\left(\sum_{j\in\Lambda_e}\mathscr{K}^{\rho}_{e,j}(\mathbf{x})\Delta x_{e,j}\right)\sum_{i\in\Lambda_e}\psi^{(0)}_{e.i}(\mathbf{x})=1. \tag{3.43}$$

Note that it is not necessary to require the global partition polynomials, $\{\psi^{(0)}_{e,i}\}_{i\in\Lambda_e}$, to form a partition of unity.

Moreover, we construct higher order RKEM bases as

$$\Psi^{(1)}_I(\mathbf{x})=(\mathbf{x}-\mathbf{x}_I)\Psi^{(0)}_I(\mathbf{x}), \tag{3.44}$$

$$\Psi^{(2)}_I(\mathbf{x})=\frac{1}{2}(\mathbf{x}-\mathbf{x}_I)^2\Psi^{(0)}_I(\mathbf{x}), \tag{3.45}$$

$$\cdots\cdots$$

$$\Psi^{(\ell)}_I(\mathbf{x})=\frac{1}{\ell!}(\mathbf{x}-\mathbf{x}_I)^{\ell}\Psi^{(0)}_I(\mathbf{x}), \tag{3.46}$$

where $I\in\Lambda_P$.

The proposed RKEM I^m/C^n interpolation hierarchy can be written as

$$\mathscr{I}^m f=\sum_{I\in\Lambda_P}\left(\Psi^{(0)}_I(\mathbf{x})f_I+\Psi^{(1)}_I(\mathbf{x})Df\Big|_I+\cdots+\Psi^{(m)}_I(\mathbf{x})D^m f\Big|_I\right). \tag{3.47}$$

In this construction, $m=q$, which means that the globally conforming interpolants are only capable of reproducing a complete mth order polynomials.

The main result of this interpolation is summarized in the following proposition:

Proposition 3.1. *Assume that* $\exists\psi^{(0)}_{e,i}(\mathbf{x})\ \forall e\in\Lambda_E,\ i\in\Lambda_e$, *such that*

$$D^{\alpha}\psi^{(0)}_{e,i}|_{\mathbf{x}=\mathbf{x}_j}=\delta_{\alpha 0}\delta_{ij},\quad |\alpha|\leqslant\ell, i,j\in\Lambda_e \tag{3.48}$$

and define,

$$\Psi^{(0)}_I(\mathbf{x})=\mathop{\mathbf{A}}_{e\in\Lambda_E}\left(\sum_{j\in\Lambda_e}\mathscr{K}^{\rho}_{e,j}(\mathbf{x})\Delta x_{e,j}\right)\psi^{(0)}_{e.i}(\mathbf{x}), \tag{3.49}$$

$$\Psi^{(1)}_I=(\mathbf{x}-\mathbf{x}_I)\Psi^{(0)}_I(\mathbf{x}), \tag{3.50}$$

$$\Psi^{(2)}_I=\frac{1}{2!}(\mathbf{x}-\mathbf{x}_I)^2\Psi^{(0)}_I(\mathbf{x}), \tag{3.51}$$

$$\cdots\cdots$$

$$\Psi^{(\ell)}_I=\frac{1}{\ell!}(\mathbf{x}-\mathbf{x}_I)^{\ell}\Psi^{(0)}_I(\mathbf{x}), \tag{3.52}$$

where $(e,i)\to I$ *and*

$$\sum_{I\in\Lambda_P}\Psi^{(0)}_I(\mathbf{x}):=\mathop{\mathbf{A}}_{e\in\Lambda_E}\left(\sum_{j\in\Lambda_e}\mathscr{K}^{\rho}_{e,j}(\mathbf{x})\Delta x_{e,j}\right)\left(\sum_{i\in\Lambda_e}\psi^{(0)}_{e.i}(\mathbf{x})\right)=1. \tag{3.53}$$

The interpolation scheme (3.47) *has the following properties:*

1. $D^{\alpha}\Psi^{(\beta)}_I|_{\mathbf{x}=\mathbf{x}_J}=\delta_{\alpha\beta}\delta_{IJ},\ I,J\in\Lambda_P,\ |\alpha|,|\beta|\leqslant m$;
2. $\mathscr{I}^m\mathbf{x}^{\lambda}=\mathbf{x}^{\lambda}\ \forall\mathbf{x}\in\Omega,\ |\lambda|\leqslant m$.

Proof. We first show that $D^\alpha \Psi_I^{(0)}|_{\mathbf{x}=\mathbf{x}_J} = \delta_{\alpha 0}\delta_{IJ}$, $|\alpha| \leqslant m$.

By the product rule,

$$\begin{aligned} D^\alpha \Psi_I^{(0)}|_{\mathbf{x}=\mathbf{x}_J} &= D^\alpha \left\{ \mathop{\mathbf{A}}_{e\in\Lambda_E} \left[\left(\sum_{j\in\Lambda_e} \mathscr{K}^\rho_{e,j}(\mathbf{x})\Delta\mathbf{x}_{e,j} \right) \psi^{(0)}_{e,i}(\mathbf{x}) \right] \right\} \Bigg|_{\mathbf{x}=\mathbf{x}_J} \\ &= \mathop{\mathbf{A}}_{e\in\Lambda_E} \left\{ \sum_{|\gamma|\leqslant|\alpha|} \binom{\alpha}{\gamma} \left(\sum_{j\in\Lambda_e} D^{\alpha-\gamma}\mathscr{K}^\rho_{e,j}(\mathbf{x})\Delta\mathbf{x}_{e,j} \right) \left(D^\gamma \psi^{(0)}_{e,i}(\mathbf{x}) \right) \right\} \Bigg|_{\mathbf{x}=\mathbf{x}_J} \\ &= \mathop{\mathbf{A}}_{e\in\Lambda_E} \left\{ \sum_{|\gamma|\leqslant|\alpha|} \binom{\alpha}{\gamma} \delta_{\gamma 0}\delta_{IJ} \left(\sum_{j\in\Lambda_e} D^{\alpha-\gamma}\mathscr{K}^\rho_{e,j}(\mathbf{x})\Delta\mathbf{x}_{e,j} \right) \right\} \Bigg|_{\mathbf{x}=\mathbf{x}_J}. \end{aligned} \tag{3.54}$$

Note that in line 3, Eq. (3.48) is used if $\mathbf{x}_J$ is a nodal point of Ω_e. If $\mathbf{x}_J$ is not a nodal point of Ω_e, by locality of meshfree basis functions,

$$\mathbf{x}_J \notin \overline{\Omega}_e \Rightarrow \mathbf{x}_J \notin \bigcup_{j\in\Lambda_e} \operatorname{supp}\{\mathscr{K}^\rho_{e,j}\} \tag{3.55}$$

and therefore, we have the term δ_{IJ} instead of δ_{Ij}. A pictorial illustration of this point is shown in Fig. 2.

Since the terms associated with $\gamma \neq 0$ are all 0, the only non-zero term left in (3.54) is the term corresponding to $\gamma = 0$. Consider $\binom{\alpha}{0} = 1$. We have

$$D^\alpha \Psi_I^{(0)}\Big|_{\mathbf{x}=\mathbf{x}_J} = \delta_{IJ} \mathop{\mathbf{A}}_{e\in\Lambda_E} \left\{ \sum_{j\in\Lambda_e} D^\alpha \mathscr{K}^\rho_{e,j}(\mathbf{x})\Delta\mathbf{x}_{e,j} \right\} \Bigg|_{\mathbf{x}=\mathbf{x}_J} \tag{3.56}$$

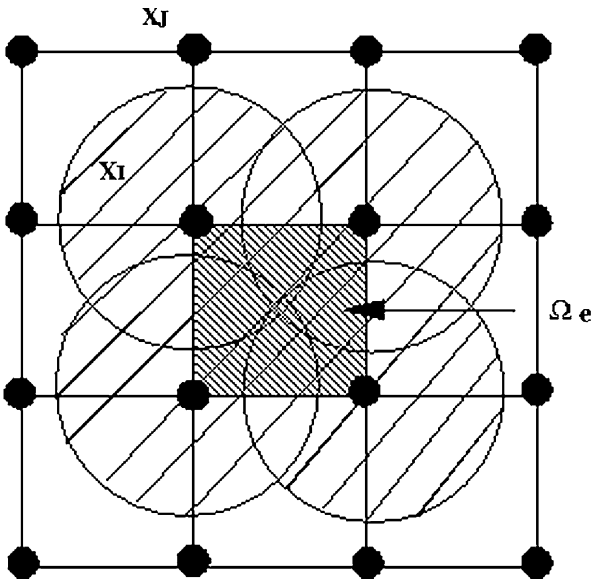

Fig. 2. A pictorial proof of $\mathbf{x}_J \notin \overline{\Omega}_e \Rightarrow \mathbf{x}_J \notin \bigcup_{j\in\Lambda_e} \operatorname{supp}\{\mathscr{K}^\rho_{e,j}\}$.

and we now show that

$$\mathop{\mathbf{A}}_{e\in\Lambda_E}\left\{\sum_{j\in\Lambda_e} D^{\alpha}\mathscr{K}^{\rho}_{e,j}(\mathbf{x})\Delta\mathbf{x}_{e,j}\right\}\Bigg|_{\mathbf{x}=\mathbf{x}_J}=\delta_{\alpha 0}.$$

Even though in general,

$$\sum_{i\in\Lambda_e}\psi^{(0)}_{e,i}(\mathbf{x})\neq 1,$$

but at the nodal point, Kronecker delta property ensures that

$$\sum_{i\in\Lambda_e}\psi^{(0)}_{e,i}(\mathbf{x})|_{\mathbf{x}=\mathbf{x}_J}=1. \tag{3.57}$$

Consider the partition of unity condition (3.53).

$$\mathop{\mathbf{A}}_{e\in\Lambda_E}\left[\sum_{j\in\Lambda_e}\mathscr{K}^{\rho}_{e,j}(\mathbf{x})\Delta\mathbf{x}_{e,j}\right]\left[\sum_{i\in\Lambda_e}\psi^{(0)}_{e,i}(\mathbf{x})\right]=1. \tag{3.58}$$

It implies that

$$\mathop{\mathbf{A}}_{e\in\Lambda_E}\left\{\sum_{j\in\Lambda_e} D^{\alpha}\mathscr{K}^{\rho}_{e,j}(\mathbf{x})\Delta\mathbf{x}_{e,j}\right\}\Bigg|_{\mathbf{x}=\mathbf{x}_J}=1,\quad\text{when}\quad\alpha=0. \tag{3.59}$$

When $\alpha\neq 0$, differentiation of (3.58) yields,

$$\begin{aligned}
D^{\alpha}\mathop{\mathbf{A}}_{e\in\Lambda_E}\left\{\sum_{j\in\Lambda_e}\mathscr{K}^{\rho}_{e,j}(\mathbf{x})\Delta\mathbf{x}_{e,j}\right\}\Bigg|_{\mathbf{x}=\mathbf{x}_J} &= \mathop{\mathbf{A}}_{e\in\Lambda_E}\left\{\sum_{|\gamma|\leqslant|\alpha|}\binom{\alpha}{\gamma}\left[\sum_{j\in\Lambda_e}D^{\alpha-\gamma}\mathscr{K}^{\rho}_{e,j}(\mathbf{x})\Delta\mathbf{x}_{e,j}\right]\left[\sum_{i\in\Lambda_e}D^{\gamma}\psi^{(0)}_{e,i}(\mathbf{x})\right]\right\}\Bigg|_{\mathbf{x}=\mathbf{x}_J}\\
&= \mathop{\mathbf{A}}_{e\in\Lambda_E}\left\{\sum_{|\gamma|\leqslant|\alpha|}\binom{\alpha}{\gamma}\left[\sum_{j\in\Lambda_e}D^{\alpha-\gamma}\mathscr{K}^{\rho}_{e,j}(\mathbf{x})\Delta\mathbf{x}_{e,j}\right]\Bigg|_{\mathbf{x}=\mathbf{x}_J}\left[\delta_{\gamma 0}\delta_{IJ}\right]\right\}\\
&= \delta_{IJ}\mathop{\mathbf{A}}_{e\in\Lambda_E}\left\{\binom{\alpha}{0}\left[\sum_{j\in\Lambda_e}D^{\alpha}\mathscr{K}^{\rho}_{e,j}(\mathbf{x})\Delta\mathbf{x}_{e,j}\right]\right\}\Bigg|_{\mathbf{x}=\mathbf{x}_J}=0\\
&\Rightarrow \mathop{\mathbf{A}}_{e\in\Lambda_E}\left\{\sum_{j\in\Lambda_e} D^{\alpha}\mathscr{K}^{\rho}_{e,j}(\mathbf{x})\Delta\mathbf{x}_{e,j}\right\}\Bigg|_{\mathbf{x}=\mathbf{x}_J}=0,\quad\text{when}\quad\alpha\neq 0.
\end{aligned} \tag{3.60}$$

We now show that

$$D^{\alpha}\Psi^{(\beta)}_I(\mathbf{x})\Big|_{\mathbf{x}=\mathbf{x}_J}=\delta_{\alpha\beta}\delta_{IJ},\quad\text{when}\quad\beta\neq 0, \tag{3.61}$$

where $\Psi^{(\beta)}_I(\mathbf{x})=\frac{(\mathbf{x}-\mathbf{x}_I)^{\beta}}{\beta!}\Psi^{(0)}_I(\mathbf{x})$.

It is readily to show that

$$\begin{aligned}
D^{\alpha}\Psi^{(\beta)}_I(\mathbf{x}) &= \sum_{|\gamma|<|\alpha|}\binom{\alpha}{\gamma}D^{\alpha-\gamma}\Psi^{(0)}_I(\mathbf{x})D^{\gamma}\left((\mathbf{x}-\mathbf{x}_I)^{\beta}\right)\\
&= \sum_{|\gamma|\leqslant|\alpha|}\left(\binom{\alpha}{\gamma}D^{\alpha-\gamma}\Psi^{(0)}_I(\mathbf{x})\frac{\beta!}{(\beta-\gamma-1)!\beta!}(\mathbf{x}-\mathbf{x}_I)^{\langle\beta-\gamma\rangle}\right)\Bigg|_{\mathbf{x}=\mathbf{x}_J},
\end{aligned} \tag{3.62}$$

where

$$\langle \beta-\gamma\rangle = \begin{cases} \beta-\gamma, & |\beta-\gamma| \geqslant 0, \\ 0, & |\beta-\gamma| < 0. \end{cases} \tag{3.63}$$

Consequently,

$$\begin{aligned} D^{\alpha}\Psi_I^{(\beta)}(\mathbf{x}_J) &= \sum_{|\gamma|\leqslant|\alpha|} \binom{\alpha}{\gamma} D^{\alpha-\gamma}\Psi_I^{(0)}(\mathbf{x}) \frac{1}{(\beta-\gamma)!}(\mathbf{x}-\mathbf{x}_I)^{\langle\beta-\gamma\rangle}\Big|_{\mathbf{x}=\mathbf{x}_J} \\ &= \sum_{|\gamma|\leqslant|\alpha|} \binom{\alpha}{\gamma} \delta_{\alpha-\beta 0}\delta_{IJ} \frac{1}{(\beta-\gamma)!}(\mathbf{x}_J-\mathbf{x}_I)^{\langle\beta-\gamma\rangle} \\ &= \binom{\alpha}{\beta}\delta_{\alpha\beta}\delta_{IJ} = \delta_{\alpha\beta}\delta_{IJ}. \end{aligned} \tag{3.64}$$

We now show that $\mathscr{I}\mathbf{x}^{\lambda} = \mathbf{x}^{\lambda}$. By construction $|\lambda| < m$,

$$\begin{aligned} \mathscr{I}\mathbf{x}^{\lambda} = \sum_{I\in\Lambda_P} \Big(& \Psi_I^{(0)}(\mathbf{x})\mathbf{x}^{\lambda} + \Psi_I^{(1)}(\mathbf{x})\lambda\mathbf{x}^{\langle\lambda-1\rangle} + \cdots + \Psi_I^{(\gamma)}(\mathbf{x})\lambda(\lambda-1)\cdots(\lambda-\gamma+1)\mathbf{x}_I^{\langle\lambda-\gamma\rangle} \\ & + \cdots + \Psi_I^{(m)}(\mathbf{x})\lambda(\lambda-1)\cdots(\lambda-m+1)\mathbf{x}_I^{\langle\lambda-m\rangle}\Big). \end{aligned} \tag{3.65}$$

Consider $\Psi_I^{(\gamma)}(\mathbf{x}) := \frac{1}{\gamma!}(\mathbf{x}-\mathbf{x}_I)^{\gamma}\Psi_I^{(0)}(\mathbf{x})$ and the last term $\langle\lambda-\gamma\rangle \geqslant 0$ is the term $\gamma = \lambda$. We then have

$$\begin{aligned} \mathscr{I}\mathbf{x}^{\lambda} &= \sum_{I\in\Lambda_P} \Psi_I^{(0)}(\mathbf{x})\left(\binom{\lambda}{0}\mathbf{x}_I^{\lambda} + \binom{\lambda}{1}\mathbf{x}_I^{\lambda-1}(\mathbf{x}-\mathbf{x}_I) + \cdots + \binom{\lambda}{\gamma}\mathbf{x}_I^{\lambda-\gamma}(\mathbf{x}-\mathbf{x}_I)^{\gamma} + \cdots + \binom{\lambda}{\lambda}(\mathbf{x}-\mathbf{x}_I)^{\lambda}\right) \\ &= \sum_{I\in\Lambda_P} \Psi_I^{(0)}(\mathbf{x})\left(\sum_{|\gamma|\leqslant|\lambda|} \binom{\lambda}{\gamma}\mathbf{x}_I^{\lambda-\gamma}(\mathbf{x}-\mathbf{x}_I)^{\gamma}\right) = \sum_{I\in\Lambda_P}\Psi_I^{(0)}(\mathbf{x})\mathbf{x}^{\lambda} = \mathbf{x}^{\lambda}, \end{aligned} \tag{3.66}$$

where the partition of unity condition $\sum_{I\in\Lambda_P}\Psi_I^{(0)}(\mathbf{x}) = 1$ is used. □

3.2. 1D I^2/C^n interpolation

Let $\xi = (x-x_e)/L_e$ and $L_e = x_{e+1}-x_e$. The two nodes I^2 FEM Hermite interpolations are

$$\begin{cases} H_1^{(0)}(\xi) = 1 - 10\xi^3 + 15\xi^4 - 6\xi^5, \\ H_2^{(0)}(\xi) = 10\xi^3 - 15\xi^4 + 6\xi^5, \end{cases} \tag{3.67}$$

$$\begin{cases} H_1^{(1)}(\xi) = L_e(\xi - 6\xi^3 + 8\xi^4 - 3\xi^5), \\ H_2^{(1)}(\xi) = L_e(-4\xi^3 + 7\xi^4 - 3\xi^5), \end{cases} \tag{3.68}$$

$$\begin{cases} H_1^{(2)}(\xi) = \dfrac{L_e^2}{2}(\xi^2 - 3\xi^3 + 3\xi^4 - \xi^5), \\ H_2^{(1)}(\xi) = \dfrac{L_e^2}{2}(\xi^3 - 2\xi^4 - \xi^5). \end{cases} \tag{3.69}$$

The fifth order Hermite interpolants satisfy the following ten interpolation conditions,

$$\text{partition of unity:} \quad \sum_{i=1}^{2} H_{e,i}^{(0)}(x) = 1, \tag{3.70}$$

$$\left.\frac{\mathrm{d}^{\alpha}H^{(\beta)}_{e,i}}{\mathrm{d}x^{\alpha}}\right|_{x=x_j}=\delta_{\alpha\beta}\delta_{ij},\quad i,j=1,2;\ \ 0\leqslant\alpha,\ \ \beta\leqslant 2. \tag{3.71}$$

Suppose that the finite element connectivity map has the form

$$\Lambda_E\times\Lambda_e\to\Lambda_P:(e_1,i_1),(e_2,i_\ell)\to I. \tag{3.72}$$

Note that $\ell=1,2$. In the interior $\ell=2$ and on the boundary $\ell=1$.

The fifth order RKEM Hermite interpolants are constructed as follows:

$$\Psi^{(0)}_I(x)=\sum_{k=1}^{\ell}\left(\sum_{j\in\Lambda_{e_k}}\mathscr{K}^{\varrho}_{e_k,j}(x)\Delta x_{e_k,j}\right)H^{(0)}_{e_k,i_k}(x), \tag{3.73}$$

$$\Psi^{(1)}_I(x)=\sum_{k=1}^{\ell}\left(\sum_{j\in\Lambda_{e_k}}\mathscr{K}^{\varrho}_{e_k,j}(x)\Delta x_{e_k,j}\right)(x-x_I)H^{(0)}_{e_k,i_k}(x), \tag{3.74}$$

$$\Psi^{(2)}_I(x)=\sum_{k=1}^{\ell}\left(\sum_{j\in\Lambda_{e_k}}\mathscr{K}^{\varrho}_{e_k,j}(x)\Delta x_{e_k,j}\right)\frac{(x-x_I)^2}{2!}H^{(0)}_{e_k,i_k}(x). \tag{3.75}$$

The hybrid RKEM Hermite interpolation can be expressed as

$$\mathscr{I}u(x)=\sum_{I\in\Lambda_P}\left(\Psi^{(0)}_I(x)u_I+\Psi^{(1)}_I(x)u'_I+\Psi^{(2)}_I(x)u''_I\right), \tag{3.76}$$

where $u'_I:=\frac{\mathrm{d}u}{\mathrm{d}x}|_{x=x_I}$ and $u''_I:=\frac{\mathrm{d}^2u}{\mathrm{d}x^2}|_{x=x_I}$.

Again we choose cubic spline as meshfree window function. All three I^2/C^n RKEM shape functions and their derivatives are plotted in Fig. 3.

The proposed I^2/C^n RKEM Hermite interpolants satisfy the 10 Hermite interpolation conditions and can reproduce polynomial, x^{λ}, $\lambda=0,1,2$.

3.3. 2D I^0/C^n quadrilateral RKEM

We now consider a two-dimensional I^0 quadrilateral element (see Fig. 4(a)). By nodal integration (trapezoidal rule),

$$\int_{\Omega_e}\mathscr{K}_{\varrho}(\mathbf{y}-\mathbf{x};\mathbf{x})\,\mathrm{d}\mathbf{y}\approx\frac{\Delta V_e}{4}\left(\mathscr{K}^{\varrho}_{e,1}(\mathbf{x})+\mathscr{K}^{\varrho}_{e,2}(\mathbf{x})+\mathscr{K}^{\varrho}_{e,3}(\mathbf{x})+\mathscr{K}^{\varrho}_{e,4}(\mathbf{x})\right)=\sum_{j=1}^{4}\mathscr{K}^{\varrho}_{e,j}(\mathbf{x})\Delta V_{e,j}, \tag{3.77}$$

where $\Delta V_{e,j}=\frac{1}{4}\Delta V_e$, $j=1,2,3,4$, and

$$\mathscr{K}^{\rho}_{e,j}(\mathbf{x}):=\frac{1}{\varrho^2}w\left(\frac{\mathbf{x}-\mathbf{x}_{e,j}}{\varrho}\right)b(\mathbf{x}). \tag{3.78}$$

The partition of unity condition yields the equality

$$\mathop{\mathbf{A}}_{e\in\Lambda_E}\left(\sum_{j=1}^{4}\frac{\Delta V_{e,j}}{\varrho^2}w\left(\frac{\mathbf{x}-\mathbf{x}_{e,j}}{\varrho}\right)\right)b(\mathbf{x})\left(\sum_{i=1}^{4}\psi_{e,i}(\mathbf{x})\right)=1. \tag{3.79}$$

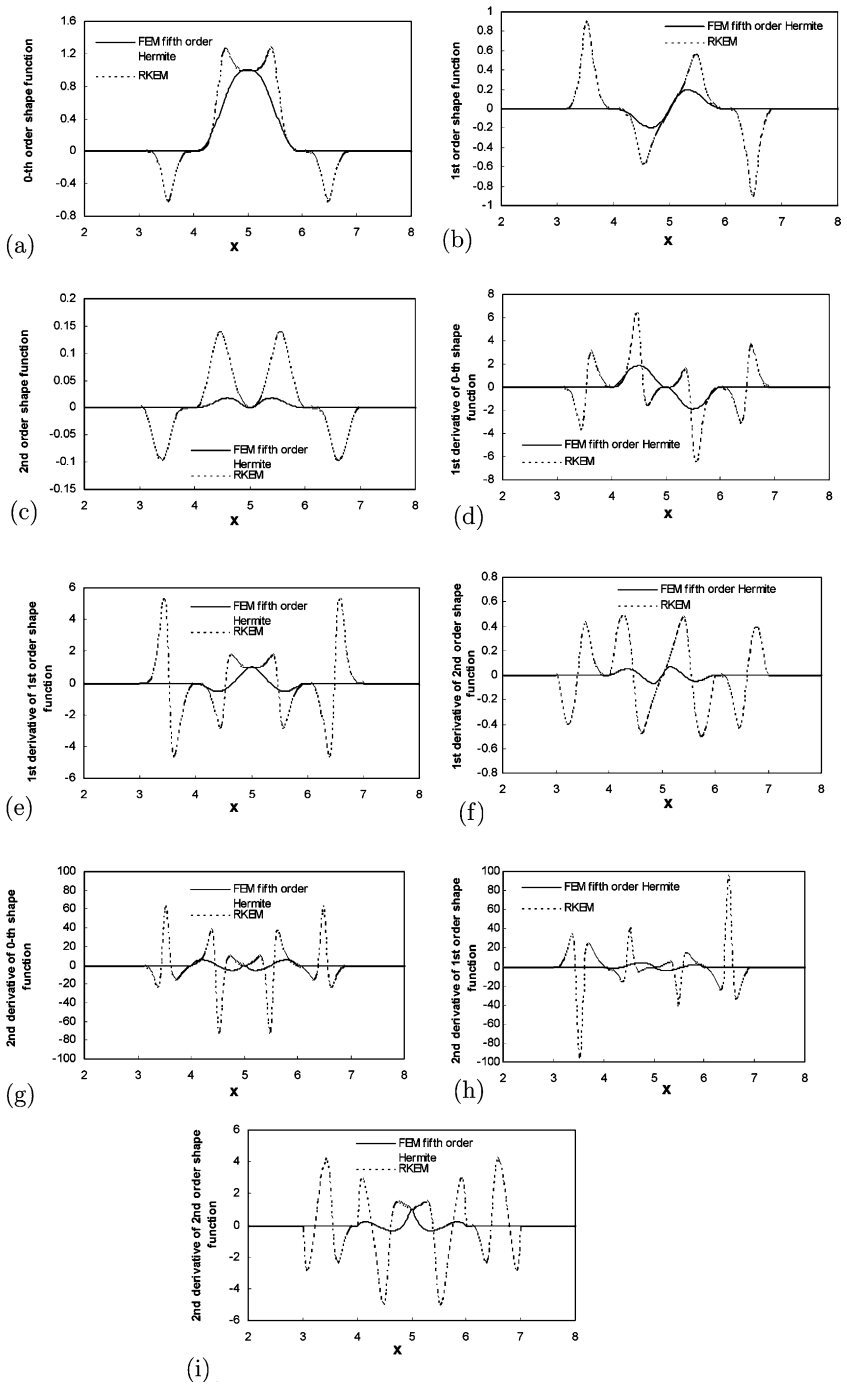

Fig. 3. An 1D I^2/C^4 RKEM interpolant: (a) shape function $\Psi_I^{(0)}(x)$, (b) shape function $\Psi_I^{(1)}(x)$, (c) shape function $\Psi_I^{(2)}(x)$, (d) the 1st derivative of $\Psi_I^{(0)}(x)$, (e) the 1st derivative of $\Psi_I^{(1)}(x)$, (f) the 1st derivative of $\Psi_I^{(2)}(x)$, (g) the 2nd derivative of $\Psi_I^{(0)}(x)$, (h) the 2nd derivative of $\Psi_I^{(1)}(x)$, and (i) the 2nd derivative of $\Psi_I^{(2)}(x)$.

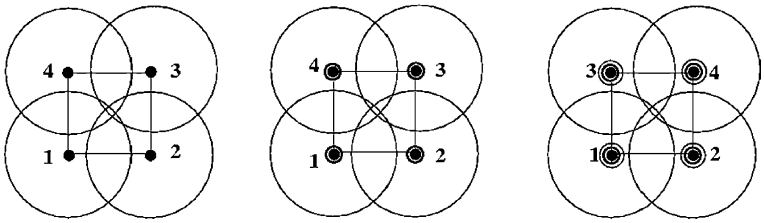

Fig. 4. Two-dimensional quadrilateral RKEM hierarchical interpolation field: (a) I^0 element, (b) I^1 element, and (c) I^2 element.

Solving $b(\mathbf{x})$, one may find that

$$\mathscr{K}^{(0)}_{e,j}(\mathbf{x}) := \frac{1}{\varrho^2} w\left(\frac{\mathbf{x}_{e,j}-\mathbf{x}}{\varrho}\right)\left\{\mathop{\mathbf{A}}_{e\in\Lambda_E}\left[\sum_{j=1}^{4}\frac{\Delta V_{e,j}}{\varrho^2} w\left(\frac{\mathbf{x}_{e,j}-\mathbf{x}}{\varrho}\right)\left(\sum_{i=1}^{4}\psi_{e,i}(\mathbf{x})\right)\right]\right\}^{-1}. \tag{3.80}$$

Consider the connectivity map

$$(e_1,i_1),\ldots,(e_k,i_k),\ldots,(e_\ell,i_\ell)\to I. \tag{3.81}$$

The two-dimensional quadrilateral reproducing kernel element shape function can be expressed as

$$\Psi^{(0)}_I(\mathbf{x}) = \sum_{k=1}^{\ell}\left(\sum_{j=1}^{4}\frac{\Delta V_{e_k,j}}{\varrho} w\left(\frac{\mathbf{x}-\mathbf{x}_{e_k,j}}{\varrho}\right)\left\{\mathop{\mathbf{A}}_{e\in\Lambda_E}\left(\sum_{j=1}^{4}\frac{\Delta V_{e,j}}{\varrho^2} w\left(\frac{\mathbf{x}-\mathbf{x}_{e,j}}{\varrho}\right)\right)\left(\sum_{i=1}^{4}\psi_{e,i}(x)\right)\right\}^{-1}\psi_{e_k,i_k}(\mathbf{x})\right). \tag{3.82}$$

For element e with four nodes (x_1,y_1), (x_2,y_2), (x_3,y_3), (x_4,y_4), and the global partition shape functions are:

$$\psi_{e,1}(\xi(\mathbf{x}),\eta(\mathbf{x})) = \tfrac{1}{4}(1-\xi)(1-\eta), \tag{3.83}$$

$$\psi_{e,2}(\xi(\mathbf{x}),\eta(\mathbf{x})) = \tfrac{1}{4}(1+\xi)(1-\eta), \tag{3.84}$$

$$\psi_{e,3}(\xi(\mathbf{x}),\eta(\mathbf{x})) = \tfrac{1}{4}(1+\xi)(1+\eta), \tag{3.85}$$

$$\psi_{e,4}(\xi(\mathbf{x}),\eta(\mathbf{x})) = \tfrac{1}{4}(1-\xi)(1+\eta) \tag{3.86}$$

with $-\infty<\xi,\eta<\infty$ and functions $\xi(\mathbf{x})$ and $\eta(\mathbf{x})$ can be found by its inverse relationship,

$$\mathbf{x} = \sum_{i=1}^{4}\psi_{e,i}(\boldsymbol{\xi})\mathbf{x}_{e,i}. \tag{3.87}$$

3.4. Globally compatible quadrilateral element Q12P1I1 element

This is a multiple dimensional compatible I^1 Hermite interpolant. It only has the minimal 12 degrees of freedom over four nodes. It is an I^1 interpolation, i.e. the first order of derivatives are sampled. If the fifth order spline is chosen as the meshfree window function, its smoothness is actually C^4.

Consider a four-nodes quadrilateral element. Choosing the same meshfree kernel function as in Eq. (3.80), except that

$$\psi^{(0)}_{e,1}(\mathbf{x}) = H^{(0)}_{c1}(\xi)H^{(0)}_{c1}(\eta), \tag{3.88}$$

$$\psi^{(0)}_{e,2}(\mathbf{x}) = H^{(0)}_{c2}(\xi)H^{(0)}_{c1}(\eta), \tag{3.89}$$

$$\psi^{(0)}_{e,3}(\mathbf{x}) = H^{(0)}_{c2}(\xi)H^{(0)}_{c2}(\eta), \tag{3.90}$$

$$\psi^{(0)}_{e,4}(\mathbf{x}) = H^{(0)}_{c1}(\xi)H^{(0)}_{c2}(\eta), \tag{3.91}$$

where $H^{(0)}_{c1}(\zeta) = 1 - 3\zeta^2 + 2\zeta^3$, $H^{(0)}_{c2}(\zeta) = 3\zeta^2 - 2\zeta^3$, and $\zeta = \xi$ and η.

The coordinate transformation are bilinear, i.e.

$$x(\xi,\eta) = \alpha_0 + \alpha_1\xi + \alpha_2\eta + \alpha_3\xi\eta, \tag{3.92}$$

$$y(\xi,\eta) = \beta_0 + \beta_1\xi + \beta_2\eta + \beta_3\xi\eta, \tag{3.93}$$

where α_i and β_i, $i = 1,2,3$ are found to be

$$\begin{cases} \alpha^e_0 = x_{e,1}, \\ \alpha^e_1 = x_{e,2} - x_{e,1}, \\ \alpha^e_2 = x_{e,4} - x_{e,1}, \\ \alpha^e_3 = x_{e,1} - x_{e,2} + x_{e,3} - x_{e,4}, \end{cases} \quad \text{and} \quad \begin{cases} \beta^e_0 = y_{e,1}, \\ \beta^e_1 = y_{e,2} - y_{e,1}, \\ \beta^e_2 = y_{e,4} - y_{e,1}, \\ \beta^e_2 = y_{e,1} - y_{e,2} + y_{e,3} - y_{e,4}. \end{cases} \tag{3.94}$$

Subsequently, one may find that the following partition polynomials,

$$x = \sum_{j=1}^{4} N_{e,j}(\xi,\eta)x_{e,j}, \quad y = \sum_{j=1}^{4} N_{e,j}(\xi,\eta)y_{e,j}, \tag{3.95}$$

where $N_{e,1}(\xi,\eta) = 1 - \xi - \eta + \xi\eta$, $N_{e,2}(\xi,\eta) = \xi(1-\eta)$, $N_{e,3}(\xi,\eta) = \xi\eta$, and $N_{e,4}(\xi,\eta) = \eta(1-\xi)$. Furthermore, it can be readily found that

$$\frac{\partial\xi}{\partial x} = \frac{1}{\Delta}(\beta_2 + \beta_3\xi), \quad \frac{\partial\xi}{\partial y} = \frac{-1}{\Delta}(\alpha_2 + \alpha_3\xi), \tag{3.96}$$

$$\frac{\partial\eta}{\partial x} = \frac{-1}{\Delta}(\beta_1 + \beta_3\eta), \quad \frac{\partial\eta}{\partial y} = \frac{1}{\Delta}(\alpha_1 + \alpha_3\eta), \tag{3.97}$$

where $\Delta = (\alpha_1 + \alpha_3\eta)(\beta_2 + \beta_3\xi) - (\alpha_2 + \alpha_3\xi)(\beta_1 + \beta_3\eta)$.

Three I^1/C^4 quadrilateral RKEM shape functions are plotted in Fig. 5.

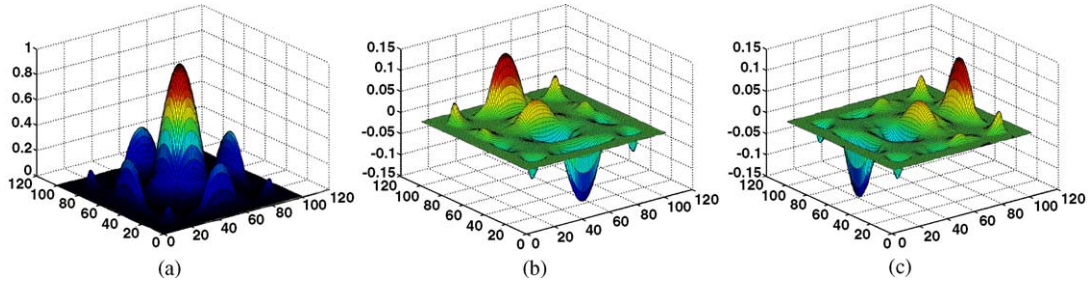

Fig. 5. Smooth quadrilateral I^1/C^4 RKEM interpolant: (a) the 1st shape function, $\Psi^{(00)}_I(\mathbf{x})$, (b) the 2nd shape function $\Psi^{(10)}_I(\mathbf{x})$, (c) the 3rd shape function $\Psi^{(01)}_I(\mathbf{x})$.

The 0th order shape functions in an element are

$$\Psi_{e,i}^{(00)}(\mathbf{x}) = \left(\sum_{j=1}^{4} \mathscr{K}_{e,j}^{\varrho}(\mathbf{x}) \Delta V_{e,j} \right) \psi_{e,i}^{(0)}(\xi,\eta), \quad i = 1,2,3,4. \tag{3.98}$$

The higher order basis functions are

$$\Psi_{e,i}^{(10)}(\mathbf{x}) = (x - x_{e,i}) \Psi_{e,i}^{(00)}(\mathbf{x}), \quad i = 1,2,3,4, \tag{3.99}$$

$$\Psi_{e,i}^{(01)}(\mathbf{x}) = (y - y_{e,i}) \Psi_{e,i}^{(00)}(\mathbf{x}), \quad i = 1,2,3,4. \tag{3.100}$$

Suppose that the finite element connectivity map has the form,

$$\Lambda_E \times \Lambda_e \to \Lambda_P : (e_1, i_1), \ldots, (e_\ell, i_\ell) \to I. \tag{3.101}$$

The 0th order global shape function has the form

$$\Psi_I^{(00)}(\mathbf{x}) = \sum_{k \in \Lambda_I} \left(\sum_{j \in \Lambda_{e_k}} \mathscr{K}_{e_k,j}^{\varrho}(\mathbf{x}) \Delta V_{e_k,j} \right) \psi_{e_k,i_k}^{(0)}(\mathbf{x}) = \sum_{k \in \Lambda_I} \Psi_{e_k,i_k}^{(00)}(\mathbf{x}), \tag{3.102}$$

where $\Lambda_I = \{1,2,\ldots,\ell\}$.

The global higher order basis functions have simple form

$$\Psi_I^{(10)}(\mathbf{x}) = (x - x_I) \Psi_I^{(00)}(\mathbf{x}), \tag{3.103}$$

$$\Psi_I^{(01)}(\mathbf{x}) = (y - y_I) \Psi_I^{(00)}(\mathbf{x}). \tag{3.104}$$

One can easily write down 16 degrees of freedom bilinear RKEM Hermite quadrilateral interpolant function by adding four additional higher order partition polynomials,

$$\Psi_{e,i}^{(11)}(\mathbf{x}) = (x - x_{e,i})(y - y_{e,i}) \Psi_{e,i}^{(00)}(\mathbf{x}), \quad i = 1,2,3,4 \tag{3.105}$$

or by adding one global shape function,

$$\Psi_I^{(11)}(\mathbf{x}) = (x - x_I)(y - y_I) \Psi_I^{(00)}(\mathbf{x}). \tag{3.106}$$

It can be easily shown that the above minimal compatible C^1 Hermite RKEM interpolants can reproduce polynomials, 1, x, y, and xy.

3.5. Globally compatible Q16P2I2 quadrilateral element

Choosing the same meshfree kernel function as in Eq. (3.80), except that

$$\psi_{e,1}^{(0)}(\mathbf{x}) = H_{f1}^{(0)}(\xi) H_{f1}^{(0)}(\eta), \tag{3.107}$$

$$\psi_{e,2}^{(0)}(\mathbf{x}) = H_{f2}^{(0)}(\xi) H_{f1}^{(0)}(\eta), \tag{3.108}$$

$$\psi_{e,3}^{(0)}(\mathbf{x}) = H_{f2}^{(0)}(\xi) H_{f2}^{(0)}(\eta), \tag{3.109}$$

$$\psi_{e,4}^{(0)}(\mathbf{x}) = H_{f2}^{(0)}(\xi) H_{f1}^{(0)}(\eta), \tag{3.110}$$

where $H_{f1}^{(0)}(\zeta) = 1 - 10\zeta^3 + 15\zeta^4 - 6\zeta^5$ and $H_{f2}^{(0)}(\zeta) = 10\zeta^3 - 15\zeta^4 + 6\zeta^5$. The coordinate transformation are bilinear, which is exactly the same as Eqs. (3.92)–(3.95).

We can construct minimal 24 degrees of freedom, compatible I^2/C^n RKEM Hermite interpolants. With the local zero-order basis functions,

$$\Psi_{e,i}^{(00)}(\mathbf{x}) = \left(\sum_{j=1}^{4} \mathscr{K}_{e,j}^{\varrho}(\mathbf{x}) \right) \psi_{e,i}^{(0)}(\mathbf{x}), \quad i = 1,2,3,4 \tag{3.111}$$

and higher order basis functions

$$\Psi_{e,i}^{(10)}(\mathbf{x}) = (x - x_{e,i}) \Psi_{e,i}^{(00)}(\mathbf{x}), \quad i = 1,2,3,4, \tag{3.112}$$

$$\Psi_{e,i}^{(01)}(\mathbf{x}) = (y - y_{e,i}) \Psi_{e,i}^{(00)}(\mathbf{x}), \quad i = 1,2,3,4 \tag{3.113}$$

and

$$\Psi_{e,i}^{(20)}(\mathbf{x}) = \tfrac{1}{2}(x - x_{e,i})^2 \Psi_{e,i}^{(00)}(\mathbf{x}), \quad i = 1,2,3,4, \tag{3.114}$$

$$\Psi_{e,i}^{(11)}(\mathbf{x}) = (x - x_{e,i})(y - y_{e,i}) \Psi_{e,i}^{(00)}(\mathbf{x}), \quad i = 1,2,3,4, \tag{3.115}$$

$$\Psi_{e,i}^{(02)}(\mathbf{x}) = \tfrac{1}{2}(y - y_{e,i})^2 \Psi_{e,i}^{(00)}(\mathbf{x}), \quad i = 1,2,3,4. \tag{3.116}$$

The six I^2/C^4 quadrilateral RKEM shape functions are plotted in Fig. 6.

Being expressed in global form, the 0th order global shape function has the form,

$$\Psi_I^{(00)}(\mathbf{x}) = \sum_{k=1}^{\ell} \Psi_{e_k,i_k}^{(00)}(\mathbf{x}), \tag{3.117}$$

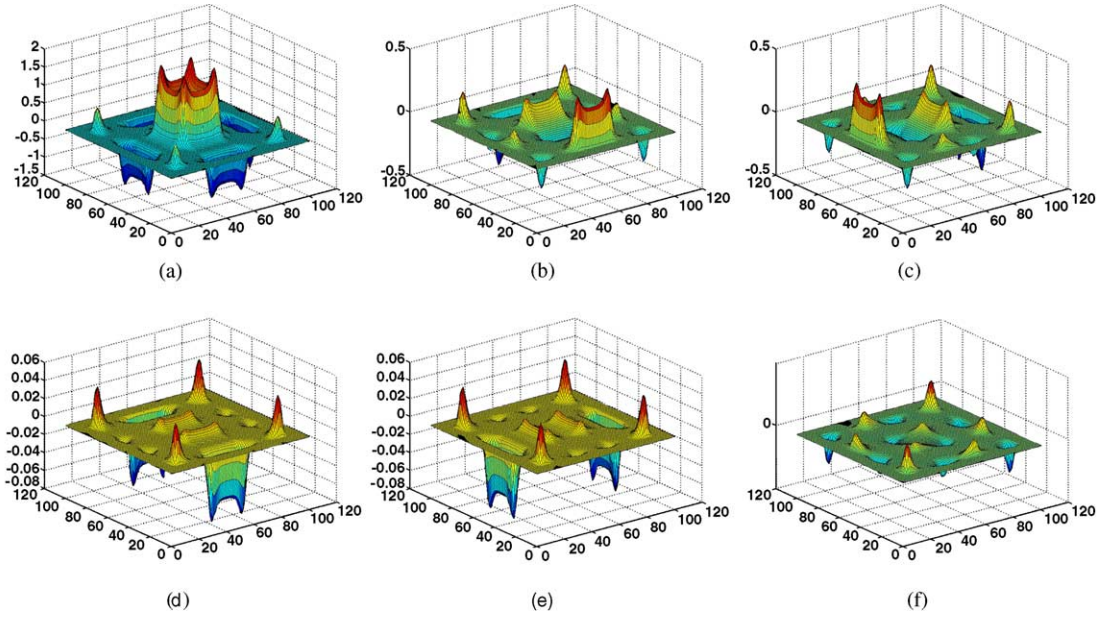

Fig. 6. Smooth quadrilateral $I^2/C^4/P^2$ RKPM interpolants: (a) the 1st shape function, $\Psi_I^{(00)}(\mathbf{x})$, (b) the 2nd shape function $\Psi_I^{(10)}(\mathbf{x})$, (c) the 3rd shape function $\Psi_I^{(01)}(\mathbf{x})$, (d) the 4th shape function $\Psi_I^{(20)}(\mathbf{x})$, (e) the 5th shape function $\Psi_I^{(02)}(\mathbf{x})$, and (f) the 6th shape function $\Psi_I^{(11)}(\mathbf{x})$.

$$\Psi_I^{(10)}(\mathbf{x}) = (x - x_I)\Psi_I^{(00)}(\mathbf{x}), \tag{3.118}$$

$$\Psi_I^{(01)}(\mathbf{x}) = (y - y_I)\Psi_I^{(00)}(\mathbf{x}), \tag{3.119}$$

$$\Psi_I^{(20)}(\mathbf{x}) = \frac{1}{2!}(x - x_I)^2\Psi_I^{(00)}(\mathbf{x}), \tag{3.120}$$

$$\Psi_I^{(11)}(\mathbf{x}) = (x - x_I)(y - y_I)\Psi_I^{(00)}(\mathbf{x}), \tag{3.121}$$

$$\Psi_I^{(02)}(\mathbf{y}) = \frac{1}{2!}(y - y_I)^2\Psi_I^{(00)}(\mathbf{x}). \tag{3.122}$$

3.6. Smooth I^0/C^n triangle RKEM

We now construct RKEM triangle elements. The meshfree particles are the same as finite element nodal points in a single element (see Fig. 7(a)). By nodal integration (Lobatto quadrature rule),

$$\int_{\Omega_e} \mathscr{K}_\varrho(\mathbf{y} - \mathbf{x}; \mathbf{x})\,\mathrm{d}\mathbf{y} \approx \frac{\Delta V_e}{3}\left(\mathscr{K}^\varrho_{e,1}(\mathbf{x}) + \mathscr{K}^\varrho_{e,2}(\mathbf{x}) + \mathscr{K}^\varrho_{e,3}(\mathbf{x})\right) = \sum_{j=1}^{3} \mathscr{K}^\varrho_{e,j}(\mathbf{x})\Delta V_{e,j}, \tag{3.123}$$

where $\Delta V_{e,j} = \frac{1}{3}\Delta V_e$, $j = 1, 2, 3$, and

$$\mathscr{K}^\varrho_{e,j}(\mathbf{x}) := \frac{1}{\varrho^2} w\left(\frac{\mathbf{x}_{e,j} - \mathbf{x}}{\varrho}\right) b(\mathbf{x}). \tag{3.124}$$

The partition of unity condition requires that

$$\mathop{\mathbf{A}}_{e\in\Lambda_E}\left(\sum_{j=1}^{3} \frac{\Delta V_e}{3\varrho^2} w\left(\frac{\mathbf{x}_{e,j} - \mathbf{x}}{\varrho}\right)\right) b(\mathbf{x})\left(\sum_{i=1}^{4} \psi^{(0)}_{e,i}(\mathbf{x})\right) = 1. \tag{3.125}$$

Subsequently, one may find that

$$\mathscr{K}^\varrho_{e,j}(\mathbf{x}) := \frac{1}{\varrho^2} w\left(\frac{\mathbf{x}_{e,j} - \mathbf{x}}{\varrho}\right)\left\{\mathop{\mathbf{A}}_{e\in\Lambda_E}\left[\sum_{j=1}^{3} \frac{\Delta V_e}{3\varrho^2} w\left(\frac{\mathbf{x}_{e,j} - \mathbf{x}}{\varrho}\right)\left(\sum_{i=1}^{3} \psi^{(0)}_{e,i}(\mathbf{x})\right)\right]\right\}^{-1}. \tag{3.126}$$

For each element, there are three nodes (x_1, y_1), (x_2, y_2), (x_3, y_3), the global partition polynomials are natural coordinates or area coordinates,

$$\psi^{(0)}_{e,i}(\mathbf{x}) = \xi_{e,i}(\mathbf{x}), \quad i = 1, 2, 3 \quad \text{and} \quad \sum_{i=1}^{3} \xi_{e,i} = 1, \tag{3.127}$$

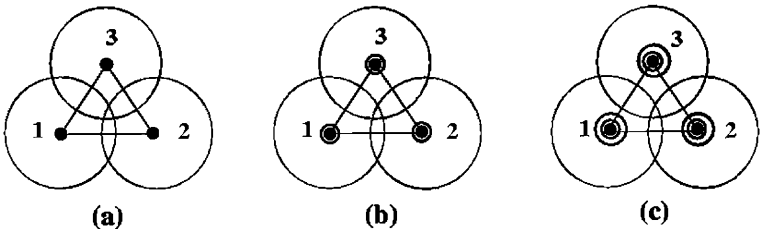

Fig. 7. Two-dimensional triangle RKEM hierarchical interpolation field: (a) I^0 element, (b) I^1 element, and (c) I^2 element.

$$\begin{bmatrix} 1 \\ x \\ y \end{bmatrix} = [\mathbf{T}] \begin{bmatrix} \xi_{e,1} \\ \xi_{e,2} \\ \xi_{e,3} \end{bmatrix} \quad \text{and} \quad \begin{bmatrix} \xi_{e,1} \\ \xi_{e,2} \\ \xi_{e,3} \end{bmatrix} = [\mathbf{T}]^{-1} \begin{bmatrix} 1 \\ x \\ y \end{bmatrix}, \tag{3.128}$$

$$[\mathbf{T}] = \begin{bmatrix} 1 & 1 & 1 \\ x_1 & x_2 & x_3 \\ y_1 & y_2 & y_3 \end{bmatrix} \quad \text{and} \quad [\mathbf{T}]^{-1} = \frac{1}{\det \mathbf{T}} \begin{bmatrix} x_2y_3 - x_3y_2 & y_{23} & x_{32} \\ x_3y_1 - x_1y_3 & y_{31} & x_{13} \\ x_1y_2 - x_2y_1 & y_{12} & x_{21} \end{bmatrix}, \tag{3.129}$$

where $\det \mathbf{T} = x_{21}y_{31} - x_{31}y_{21}$ and $x_{ij} := x_i - x_j$, $y_{ij} := y_i - y_j$.

Consider the connectivity map and by the Chain rule

$$\frac{\partial}{\partial x} = \frac{\partial}{\partial \xi_{e,i}} \frac{\partial \xi_{e,i}}{\partial x} = \frac{\epsilon_{ijk} y_{jk}}{2 \det \mathbf{T}} \frac{\partial}{\partial \xi_{e,i}}, \tag{3.130}$$

$$\frac{\partial}{\partial y} = \frac{\partial}{\partial \xi_{e,i}} \frac{\partial \xi_{e,i}}{\partial y} = \frac{\epsilon_{ijk} x_{jk}}{2 \det \mathbf{T}} \frac{\partial}{\partial \xi_{e,i}}, \tag{3.131}$$

where ϵ_{ijk} is the permutation symbol, and Einstein summation rule is implied here.

Consider the connectivity map

$$(e_1, i_1), \ldots, (e_k, i_k), \ldots, (e_\ell, i_\ell) \to I. \tag{3.132}$$

The two-dimensional triangle RKEM shape function can be expressed as

$$\Psi_I^{(0)}(\mathbf{x}) = \sum_{k=1}^{\ell} \left(\sum_{j=1}^{3} \frac{\Delta V_{e_k}}{3\varrho} w\left(\frac{\mathbf{x} - \mathbf{x}_{e_k,j}}{\varrho} \right) \left\{ \mathop{\mathbf{A}}_{e \in \Lambda_E} \left(\sum_{j=1}^{3} \frac{\Delta V_e}{3\varrho^2} w\left(\frac{\mathbf{x} - \mathbf{x}_{e,j}}{\varrho} \right) \right) \left(\sum_{i=1}^{4} \xi_{e,i}(x) \right) \right\}^{-1} \xi_{e_k,i_k}(\mathbf{x}) \right). \tag{3.133}$$

Note that again, the smoothness of the interpolant is C^n and n is the order of continuity of the window function.

3.7. Globally conforming T9P1I1 triangle element

To construct a 2D minimal, compatible, I^1, Hermite triangle, The meshfree kernel function has the same form as in Eq. (3.126), except that

$$\psi_{e,i}^{(0)}(\mathbf{x}) = 3\xi_{e,i}^2 - 2\xi_{e,i}^3, \quad i = 1, 2, 3. \tag{3.134}$$

The relationship between $\xi_{e,i} \sim x, y$ are described in Eqs. (3.128) and (3.129).

The global partition polynomials in an element satisfy the interpolation conditions:

$$\psi_{e,i}^{(0)}(\mathbf{x}_j) = \delta_{ij}; \quad \frac{\partial \psi_{e,i}^{(0)}}{\partial x}(\mathbf{x}_j) = 0, \quad \frac{\partial \psi_{e,i}^{(0)}}{\partial y}(\mathbf{x}_j) = 0. \tag{3.135}$$

Note that $\sum_{i=1}^{3} \psi_{e,i}^{(0)}(\mathbf{x}) \neq 1$. Therefore, the global partition polynomials do not form a partition of unity.

The 0th order basis functions in an element are

$$\Psi_{e,i}^{(00)}(\mathbf{x}) = \left(\sum_{j=1}^{3} \mathscr{K}_{e,j}^{\varrho}(\mathbf{x}) \Delta V_{e,j} \right) \left(3\xi_{e,i}^2 - 2\xi_{e,i}^3 \right), \quad i = 1, 2, 3. \tag{3.136}$$

The higher order bases functions in an element are

$$\Psi_{e,i}^{(10)}(\mathbf{x}) = (x - x_{e,i}) \Psi_{e,i}^{(00)}(\mathbf{x}), \quad i = 1, 2, 3, \tag{3.137}$$

$$\Psi_{e,i}^{(01)}(\mathbf{x}) = (y - y_{e,i})\Psi_{e,i}^{(00)}(\mathbf{x}), \quad i = 1,2,3. \tag{3.138}$$

The element has a minimal 9 degrees of freedom. One can show that the higher order basis functions satisfy the following interpolation properties,

$$\Psi_{e,i}^{(10)}(\mathbf{x}_i) = 0 \quad \text{and} \quad \Psi_{e,i}^{(01)}(\mathbf{x}_i) = 0 \qquad \forall i = 1,2,3, \tag{3.139}$$

$$\left.\frac{\partial \Psi_{e,i}^{(10)}}{\partial x}\right|_{\mathbf{x}=\mathbf{x}_j} = \delta_{ij}, \quad \left.\frac{\partial \Psi_{e,i}^{(01)}}{\partial x}\right|_{\mathbf{x}=\mathbf{x}_j} = 0, \qquad i,j = 1,2,3, \tag{3.140}$$

$$\left.\frac{\partial \Psi_{e,i}^{(10)}}{\partial y}\right|_{\mathbf{x}=\mathbf{x}_j} = 0, \quad \left.\frac{\partial \Psi_{e,i}^{(01)}}{\partial y}\right|_{\mathbf{x}=\mathbf{x}_j} = \delta_{ij}, \qquad i,j = 1,2,3. \tag{3.141}$$

Suppose that the finite element connectivity map has the form,

$$\Lambda_E \times \Lambda_e \to \Lambda_P : (e_1, i_1), \ldots, (e_\ell, i_\ell) \to I. \tag{3.142}$$

The 0th order global shape function has the form

$$\Psi_I^{(00)}(\mathbf{x}) = \sum_{k \in \Lambda_I} \left(\sum_{j \in \Lambda_{e_k}} \mathscr{K}^{\varrho}_{e_k,j}(\mathbf{x}) \Delta V_{e_k,j} \right) \psi^{(0)}_{e_k,i_k}(\mathbf{x}). \tag{3.143}$$

The global higher order basis functions have very simple form

$$\Psi_I^{(10)}(\mathbf{x}) = (x - x_I)\Psi_I^{(00)}(\mathbf{x}), \tag{3.144}$$

$$\Psi_I^{(01)}(\mathbf{x}) = (y - y_I)\Psi_I^{(00)}(\mathbf{x}). \tag{3.145}$$

The interpolation formula is

$$\mathscr{I}^1 f(\mathbf{x}) = \sum_{I \in \Lambda} \left(\Psi_I^{(00)}(\mathbf{x}) f_I + \Psi_I^{(10)}(\mathbf{x}) f_{Ix} + \Psi_I^{(01)}(\mathbf{x}) f_{Iy} \right). \tag{3.146}$$

The interpolation scheme (3.146) can reproduce 2D linear polynomial exactly, i.e. $\mathscr{I}^1 f(\mathbf{x}) = f(\mathbf{x})$ if $f(\mathbf{x}) = a + bx + cy$.

Remark 3.2. There is an alternative approach that can restore the partition of unity property for the global partition polynomials. Let,

$$\begin{aligned} \psi_{e,1}^{(0)} &= 3\xi_{e,1}^2 - 2\xi_{e,1}^3, \\ \psi_{e,2}^{(0)} &= 3\xi_{e,2}^2 - 2\xi_{e,2}^3, \\ \psi_{e,3}^{(0)} &= 1 - \psi_{e,1}^{(0)} - \psi_{e,2}^{(0)}. \end{aligned} \tag{3.147}$$

It is easy to verify that $\sum_{i=1}^3 \psi_{e,i}^{(0)}(\mathbf{x}) = 1$.

3.8. Globally compatible T18P2I2 triangle element

Construct meshfree kernel function as formulated in Eq. (3.126), in which we choose

$$\psi_{e,i}^{(0)}(\mathbf{x}) = 10\xi_{e,i}^3 - 15\xi_{e,i}^4 + 6\xi_{e,i}^5, \quad e \in \Lambda_E, \ \ i = 1,2,3. \tag{3.148}$$

Again, natural (area) coordinate is chosen to describe FEM shape functions, where $0 \leqslant \xi_{e,i} \leqslant 1$ are the relationship between $\xi_{e,i} \sim x, y$ are given in Eqs. (3.128) and (3.129).

The global partition polynomials in an element satisfy the following interpolation conditions $\forall i, j = 1, 2, 3$:

$$\psi^{(0)}_{e,i}(\mathbf{x}_j) = \delta_{ij}, \tag{3.149}$$

$$\frac{\partial \psi^{(0)}_{e,i}}{\partial x}(\mathbf{x}_j) = 0, \quad \frac{\partial \psi^{(0)}_{e,i}}{\partial y}(\mathbf{x}_j) = 0, \tag{3.150}$$

$$\frac{\partial^2 \psi^{(0)}_{e,i}}{\partial x^2}(\mathbf{x}_j) = 0, \quad \frac{\partial^2 \psi^{(0)}_{e,i}}{\partial x \partial y}(\mathbf{x}_j) = 0, \quad \frac{\partial^2 \psi^{(0)}_{e,i}}{\partial y^2}(\mathbf{x}_j) = 0. \tag{3.151}$$

Note that if (3.148) is used, the global partition polynomial may not be a partition of unity, i.e. $\sum_{i=1}^{3} \psi^{(0)}_{e,i}(\mathbf{x}) \neq 1$. Nevertheless, the scheme should work theoretically. If one chooses $\psi^{(0)}_{e,i}(\mathbf{x}) = 10\xi^3_{e,i} - 15\xi^4_{e,i} + 6\xi^5_{e,i}$, $i = 1, 2, e \in \Lambda_E$ and $\psi^{(0)}_{e,3} = 1 - \psi^{(0)}_{e,1} - \psi^{(0)}_{e,2}$, one can then recover the property of partition of unity.

The local 0th order basis functions are

$$\Psi^{(00)}_{e,i}(\mathbf{x}) = \left(\sum_{j=1}^{3} \mathscr{K}^{\varrho}_{e,j}(\mathbf{x}) \Delta V_{e,j} \right) \psi^{(0)}_{e,i}(\mathbf{x}), \quad i = 1, 2, 3. \tag{3.152}$$

The first order partition polynomial basis functions are

$$\Psi^{(10)}_{e,i}(\mathbf{x}) = (x - x_{e,i}) \Psi^{(0)}_{e,i}(\mathbf{x}), \quad i = 1, 2, 3, \tag{3.153}$$

$$\Psi^{(01)}_{e,i}(\mathbf{x}) = (y - y_{e,i}) \Psi^{(0)}_{e,i}(\mathbf{x}), \quad i = 1, 2, 3. \tag{3.154}$$

The second order partition polynomial basis functions are

$$\Psi^{(20)}_{e,i}(\mathbf{x}) = \frac{(x - x_{e,i})^2}{2!} \Psi^{(00)}_{e,i}(\mathbf{x}), \quad i = 1, 2, 3, \tag{3.155}$$

$$\Psi^{(11)}_{e,i}(\mathbf{x}) = (x - x_{e,i})(y - y_{e,i}) \Psi^{(00)}_{e,i}(\mathbf{x}), \quad i = 1, 2, 3, \tag{3.156}$$

$$\Psi^{(02)}_{e,i}(\mathbf{x}) = \frac{(y - y_{e,i})^2}{2!} \Psi^{(00)}_{e,i}(\mathbf{x}), \quad i = 1, 2, 3. \tag{3.157}$$

There are total 18 degrees of freedom.

Expressing in global form, one may write the 0th order global shape function as

$$\Psi^{(00)}_{I}(\mathbf{x}) = \sum_{k \in \Lambda_I} \left(\sum_{j \in \Lambda_{e_k}} \mathscr{K}^{\varrho}_{e_k,j}(\mathbf{x}) \Delta V_{e_k,j} \right) \psi^{(0)}_{e_k,i_k}(\mathbf{x}). \tag{3.158}$$

The first order basis functions are

$$\Psi^{(10)}_{I}(\mathbf{x}) = (x - x_I) \Psi^{(00)}_{I}(\mathbf{x}), \tag{3.159}$$

$$\Psi^{(01)}_{I}(\mathbf{x}) = (y - y_I) \Psi^{(00)}_{I}(\mathbf{x}). \tag{3.160}$$

The second order basis functions are

$$\Psi_I^{(20)}(\mathbf{x}) = \frac{1}{2!}(x - x_I)^2 \Psi_I^{(00)}(\mathbf{x}), \tag{3.161}$$

$$\Psi_I^{(11)}(\mathbf{x}) = (x - x_I)(y - y_I)\Psi_I^{(00)}(\mathbf{x}), \tag{3.162}$$

$$\Psi_I^{(02)}(\mathbf{y}) = \frac{1}{2!}(y - y_I)^2 \Psi_I^{(00)}(\mathbf{x}). \tag{3.163}$$

The compatible I^2 interpolation scheme is

$$\mathscr{I}^2 f(\mathbf{x}) = \sum_{I \in \Lambda_P} \left\{ \Psi_I^{(00)}(\mathbf{x}) f_I + \Psi_I^{(10)}(\mathbf{x}) f_{Ix} + \Psi_I^{(01)}(\mathbf{x}) f_{Iy} + \Psi_I^{(20)}(\mathbf{x}) f_{Ixx} + \Psi_I^{(11)}(\mathbf{x}) f_{Ixy} + \Psi_I^{(02)}(\mathbf{x}) f_{Iyy} \right\}. \tag{3.164}$$

One can show that the above interpolation formula has quadratic consistency.

4. Globally conforming I^m/C^n hierarchy II

The globally conforming I^m/C^n hierarchy constructed in the previous section has its limitations. The globally conforming hierarchy is in fact $I^m/C^n/P^m$. That is the reproducing property of the interpolant is limited by the interpolation index order m, or the enrichment order. It can only reproduce complete mth order polynomials. In order to achieve higher order accuracy, a second globally conforming $I^m/C^n/P^k$ $(k \geqslant m)$ hierarchy is proposed. This interpolation hierarchy can reproduce a complete kth order polynomials with $k \geqslant m$.

4.1. Construction

Assume that there exists a set of Hermite type global polynomials, $\{\psi_{e,i}^{(0)}, \psi_{e,i}^{(1)}, \ldots, \psi_{e,i}^{(m)}\}$, such that within the element e, they can reproduce λth order polynomials, i.e.

$$\sum_{i \in \Lambda_e} \left\{ \psi_{e,i}^{(0)}(\mathbf{x}) \mathbf{x}_i^{\lambda} + \lambda \psi_{e,i}^{(1)}(\mathbf{x}) \mathbf{x}_i^{\lambda-1} + \cdots + \frac{\lambda!}{(\lambda - m)!} \psi_{e,i}^{(m)}(\mathbf{x}) \mathbf{x}_i^{\lambda-m} \right\} = \mathbf{x}^{\lambda}, \quad |\lambda| \leqslant k. \tag{4.165}$$

Assume that the surjective mesh connectivity map has the form,

$$\Lambda_E \times \Lambda_e \to \Lambda_P : (e_1, i_1), \ldots, (e_\ell, i_\ell) \to I. \tag{4.166}$$

A set of global meshfree element basis functions are constructed as follows,

$$\begin{aligned}
\Psi_I^{(0)}(\mathbf{x}) &= \sum_{k=1}^{\ell} \left(\sum_{j \in \Lambda_{e_k}} \mathscr{K}_{e_k,j}^{\rho}(\mathbf{x}) \Delta V_{e_k,j} \right) \psi_{e_k,i_k}^{(0)}(\mathbf{x}), \\
\Psi_I^{(1)}(\mathbf{x}) &= \sum_{k=1}^{\ell} \left(\sum_{j \in \Lambda_{e_k}} \mathscr{K}_{e_k,j}^{\rho}(\mathbf{x}) \Delta V_{e_k,j} \right) \psi_{e_k,i_k}^{(1)}(\mathbf{x}), \\
&\cdots\cdots
\end{aligned} \tag{4.167}$$

$$\Psi_I^{(m)}(\mathbf{x}) = \sum_{k=1}^{\ell} \left(\sum_{j \in \Lambda_{e_k}} \mathscr{K}_{e_k,j}^{\rho}(\mathbf{x}) \Delta V_{e_k,j} \right) \psi_{e_k,i_k}^{(m)}(\mathbf{x}), \tag{4.168}$$

where $I \in \Lambda_P$ and

$$\mathop{\mathbf{A}}_{e\in\Lambda_E}\sum_{j\in\Lambda_e}\left(\mathscr{K}^{\rho}_{e,j}(\mathbf{x})\Delta V_{e,j}\right)=1. \tag{4.169}$$

Again, the proposed RKEM I^m/C^n interpolation scheme can be written as

$$I^m f=\sum_{I\in\Lambda_P}\left(\Psi^{(0)}_I(\mathbf{x})f_I+\Psi^{(0)}_I(\mathbf{x})Df|_I+\cdots+\Psi^{(m)}_I(\mathbf{x})D^m f|_I\right). \tag{4.170}$$

The main properties of this globally conforming I^m/C^n hierarchy are summarized in the following proposition.

Proposition 4.1. *Assume that* $\exists\{\psi^{(0)}_{e,i},\psi^{(1)}_{e,i},\ldots,\psi^{(m)}_{e,i}\}\ \forall e\in\Lambda_E, i\in\Lambda_e$, *such that*

$$1.\ D^{\alpha}\psi^{(\beta)}_{e,i}|_{\mathbf{x}=\mathbf{x}_j}=\delta_{\alpha\beta}\delta_{ij},\quad |\alpha|,|\beta|\leqslant m,\quad \text{and}\quad i,j\in\Lambda_e, \tag{4.171}$$

$$2.\ \sum_{i\in\Lambda_e}\left\{\psi^{(0)}_{e,i}(\mathbf{x})\mathbf{x}^{\lambda}_i+\lambda\psi^{(1)}_{e,i}(\mathbf{x})\mathbf{x}^{\lambda-1}_i+\cdots+\frac{\lambda!}{(\lambda-m)!}\psi^{(m)}_{e,i}(\mathbf{x})\mathbf{x}^{\lambda-m}_i\right\}=x^{\lambda}. \tag{4.172}$$

Consider the local-global connectivity map for a given mesh,

$$\Lambda_E\times\Lambda_e\to\Lambda_P:(e_1,i_1)\cdots(e_k,i_k)\cdots(e_\ell,i_\ell)\to I. \tag{4.173}$$

We construct the following hybrid meshfree/FEM shape functions,

$$\Psi^{(0)}_I(\mathbf{x})=\sum_{k=1}^{\ell}\left(\sum_{j\in\Lambda_{e_k}}\mathscr{K}^{\rho}_{e_k,j}(\mathbf{x})\Delta V_{e_k,j}\right)\psi^{(0)}_{e_k,i_k}(\mathbf{x}),$$

$$\Psi^{(1)}_I(\mathbf{x})=\sum_{k=1}^{\ell}\left(\sum_{j\in\Lambda_{e_k}}\mathscr{K}^{\rho}_{e_k,j}(\mathbf{x})\Delta V_{e_k,j}\right)\psi^{(1)}_{e_k,i_k}(\mathbf{x}),$$

$$\cdots\cdots \tag{4.174}$$

$$\Psi^{(m)}_I(\mathbf{x})=\sum_{k=1}^{\ell}\left(\sum_{j\in\Lambda_{e_k}}\mathscr{K}^{\rho}_{e_k,j}(\mathbf{x})\Delta V_{e_k,j}\right)\psi^{(m)}_{e_k,i_k}(\mathbf{x}), \tag{4.175}$$

where $I\in\Lambda_P$.

*Then the interpolation scheme (*4.170*) has the following properties,*

1. $D^{\alpha}\Psi^{(\beta)}_I|_{\mathbf{x}=\mathbf{x}_J}=\delta_{\alpha\beta}\delta_{IJ},\ I,J\in\Lambda_P,\ |\alpha|,|\beta|\leqslant m;$
2. $I^m\mathbf{x}^{\lambda}=\mathbf{x}^{\lambda}\ \forall\mathbf{x}\in\Omega,\ |\lambda|\leqslant k.$

Proof. We first show $D^{\alpha}\Psi^{(\beta)}_I|_{\mathbf{x}=\mathbf{x}_J}=\delta_{\alpha\beta}\delta_{IJ}\ \forall I,J\in\Lambda_P$. By definition,

$$\begin{aligned}\Psi^{(\beta)}_I(\mathbf{x})&=\sum_{k=1}^{\ell}\left(\sum_{j\in\Lambda_{e_k}}\mathscr{K}^{\rho}_{e_k,j}(\mathbf{x})\Delta V_{e_k,j}\right)\psi^{(\beta)}_{e_k,i_k}\Rightarrow D^{\alpha}\Psi^{(\beta)}_I(\mathbf{x})\\&=\sum_{|\gamma|\leqslant|\alpha|}\left\{\binom{\alpha}{\gamma}\sum_{k=1}^{\ell}D^{\alpha-\gamma}\left(\sum_{j\in\Lambda_{e_k}}\mathscr{K}^{\rho}_{e_k,j}(\mathbf{x})\Delta V_{e_k,j}\right)D^{\gamma}\psi^{(\beta)}_{e_k,i_k}\right\}\Bigg|_{\mathbf{x}=\mathbf{x}_J}.\end{aligned}$$

If $\mathbf{x}_J \in \Omega_{e_k}$, based on (4.171) $D^\gamma \psi^{(\beta)}_{e_k,i_k}(\mathbf{x}_J) = \delta_{\alpha\beta}\delta_{IJ}$. If $\mathbf{x}_J \notin \Omega_{e_k}$, the restriction on the support size of meshfree kernels requires that

$$\mathscr{K}^{\rho}_{e_k,i_k}(\mathbf{x}_J) \equiv 0. \tag{4.176}$$

Therefore,

$$D^\alpha \Psi^{(\beta)}_I(\mathbf{x})\Big|_{\mathbf{x}=\mathbf{x}_J} = \sum_{|\gamma|\leqslant|\alpha|} \left\{ \binom{\alpha}{\gamma} \sum_{k=1}^{\ell} D^{\alpha-\gamma} \left(\sum_{j\in\Lambda_{e_k}} \mathscr{K}^{\rho}_{e_k,j}(\mathbf{x})\Delta V_{e_k,j} \right) \delta_{IJ}\delta_{\gamma\beta} \right\}\Bigg|_{\mathbf{x}=\mathbf{x}_J}.$$

Since

$$\sum_{k=1}^{\ell} \left(\sum_{j\in\Lambda_{e_k}} \mathscr{K}^{\rho}_{e_k,j}(\mathbf{x})\Delta V_{e_k,j} \right) = 1, \tag{4.177}$$

if $|\alpha-\gamma| > 0$,

$$\sum_{k=1}^{\ell} D^{\alpha-\gamma} \left(\sum_{j\in\Lambda_{e_k}} \mathscr{K}^{\rho}_{e_k,j}(\mathbf{x})\Delta V_{e_k,j} \right) = 0. \tag{4.178}$$

That is

$$\binom{\alpha}{\gamma} \sum_{k=1}^{\ell} D^{\alpha-\gamma} \left(\sum_{j\in\Lambda_{e_k}} \mathscr{K}^{\rho}_{e_k,j}(\mathbf{x})\Delta V_{e_k,j} \right)\Bigg|_{\mathbf{x}=\mathbf{x}_J} = \delta_{\alpha\gamma}. \tag{4.179}$$

Hence

$$D^\alpha \Psi^{(\beta)}_I(\mathbf{x})\Big|_{\mathbf{x}=\mathbf{x}_J} = \delta_{\alpha\beta}\delta_{IJ}. \tag{4.180}$$

Next, we show $\mathscr{I}^m \mathbf{x}^\lambda = \mathbf{x}^\lambda$, $|\lambda| \leqslant k$. Note that here $|\lambda| < k$. $|\lambda|$ can be greater than m and in most cases it is. This is the reason why the second I^m/C^n hierarchy is more accurate.

Based on the construction,

$$\begin{aligned}
\mathscr{I}^m \mathbf{x}^\lambda &= \sum_{I\in\Lambda_P} \left(\Psi^{(0)}_I(\mathbf{x})\mathbf{x}^\lambda_I + \Psi^{(1)}_I(\mathbf{x})\lambda\mathbf{x}^{\langle\lambda-1\rangle}_I + \cdots + \frac{\lambda!}{(\lambda-\gamma)!}\Psi^{(\gamma)}_I(\mathbf{x})\mathbf{x}^{\langle\lambda-\gamma\rangle}_I + \cdots + \frac{\lambda!}{(\lambda-m)!}\Psi^{(m)}_I(\mathbf{x})\mathbf{x}^{\langle\lambda-m\rangle}_I \right) \\
&= \mathop{\mathbf{A}}_{e\in\Lambda_E} \left(\sum_{j\in\Lambda_e} \left(\mathscr{K}^{\rho}_{e,j}\Delta V_{e,j} \right) \sum_{i\in\Lambda_e} \left(\psi^{(0)}_{e,i}\mathbf{x}^\lambda_{e,i} + \psi^{(1)}_{e,i}\mathbf{x}^{\lambda-1}_{e,i} + \cdots + \frac{\lambda!}{(\lambda-\gamma)!}\psi^{(\gamma)}_{e,i}\mathbf{x}^{\langle\lambda-\gamma\rangle}_{e,i} \right.\right. \\
&\quad \left.\left. + \cdots + \frac{\lambda!}{(\lambda-m)!}\psi^{(m)}_{e,i}\mathbf{x}^{\langle\lambda-m\rangle}_{e,i} \right) \right).
\end{aligned} \tag{4.181}$$

Based on the assumptions that

1. $\displaystyle\sum_{i\in\Lambda_e} \left(\psi^{(0)}_{e,i}\mathbf{x}^\lambda_{e,i} + \cdots + \frac{\lambda!}{(\lambda-\gamma)!}\psi^{(\gamma)}_{e,i}\mathbf{x}^{\langle\lambda-\gamma\rangle}_{e,i} + \cdots + \frac{\lambda!}{(\lambda-m)!}\psi^{(m)}_{e,i}\mathbf{x}^{\langle\lambda-m\rangle}_{e,i} \right) = \mathbf{x}^\lambda,$

2. $\displaystyle\mathop{\mathbf{A}}_{e\in\Lambda_E} \sum_{j\in\Lambda_e} \left(\mathscr{K}^{\rho}_{e,j}\Delta V_{e,j} \right) = 1.$

We conclude that

$$\mathscr{I}^m \mathbf{x}^\lambda = \mathop{\mathbf{A}}_{e\in\Lambda_E} \sum_{j\in\Lambda_e} \left(\mathscr{K}^{\rho}_{e,j} \Delta V_{e,j} \right) \mathbf{x}^\lambda = \mathbf{x}^\lambda. \qquad \square \tag{4.182}$$

4.2. 1D Example: an $I^1/C^4/P^3$ interpolant

For tutorial reason, we first construct an 1D $I^1/C^4/P^3$ hybrid RKEM interpolant.

Consider a two nodes element, $e \to [x_e, x_{e+1}]$. Let $\xi = (x - x_e)/L_e$ where $L_e = x_{e+1} - x_e$. We choose 1D cubic Hermite polynomials as the global partition polynomials, which are

$$\psi^{(0)}_{e,1}(\xi) = 1 - 3\xi^2 + 2\xi^3, \quad \psi^{(0)}_{e,2}(\xi) = 3\xi^2 - 2\xi^3,$$

$$\psi^{(1)}_{e,1}(\xi) = L_e(\xi - 2\xi^2 + \xi^3), \quad \psi^{(1)}_{e,2}(\xi) = L_e(-\xi^2 + \xi^3).$$

For a sufficient smooth function $f(x)$, the hybrid RKEM interpolant is expressed as

$$\begin{aligned} \mathscr{I}^1 f(x) &= \mathop{\mathbf{A}}_{e\in\Lambda_E} \left\{ \left(\sum_{j=1}^{2} \mathscr{K}^{\rho}_{e,j}(x) \Delta x_{e,j} \right) \left(\sum_{i=1}^{2} \psi^{(0)}_{e,i}(x) f_{e,i} \right) + \left(\sum_{j=1}^{2} \mathscr{K}^{\rho}_{e,j}(x) \Delta x_{e,j} \right) \left(\sum_{i=1}^{2} \psi^{(1)}_{e,i}(x) f'_{e,i} \right) \right\} \\ &= \sum_{I\in\Lambda_P} \left(\Psi^{(0)}_I(x) f_I + \Psi^{(1)}_I(x) f'_I \right). \end{aligned} \tag{4.183}$$

Suppose that the mesh connectivity map has the form,

$$\Lambda_E \times \Lambda_e \to \Lambda_P : (e_1, i_1), (e_2, i_2) \to I.$$

The global RKEM shape functions are

$$\Psi^{(0)}_I(x) = \sum_{k=1}^{2} \left(\sum_{j\in\Lambda_{e_k}} \mathscr{K}^{\rho}_{e_k,j}(x) \Delta x_{e_k,j} \right) \psi^{(0)}_{e_k,i_k}, \tag{4.184}$$

$$\Psi^{(1)}_I(x) = \sum_{k=1}^{2} \left(\sum_{j\in\Lambda_{e_k}} \mathscr{K}^{\rho}_{e_k,j}(x) \Delta x_{e_k,j} \right) \psi^{(1)}_{e_k,i_k}. \tag{4.185}$$

In order that $\Psi^{(i)}_I \in C^4(\Omega)$, $i = 1, 2$ and $I \in \Lambda_E$, we choose the fifth order spline function as the window function of the meshfree kernel. The global shape functions and their first order derivatives are plotted in Fig. 8.

4.3. 2D example I: a globally conforming Gallagher element

In this example, we choose the global partition polynomials derived from the previous 2D incompatible rectangular element, or Gallagher element [11] (Fig. 9).

To derive the global partition polynomials, we consider the following element interpolation field in a four nodes rectangular element,

$$\mathscr{I}_{\text{loc}} f = \sum_{i=1}^{4} \psi^{(00)}_{e,i}(\mathbf{x}) f_{e,i} + \psi^{(10)}_{e,i}(\mathbf{x}) \left.\frac{\partial f}{\partial x}\right|_{e,i} + \psi^{(01)}_{e,i}(\mathbf{x}) \left.\frac{\partial f}{\partial y}\right|_{e,i} = \boldsymbol{\psi}^{\mathrm{T}} \mathbf{f}, \tag{4.186}$$

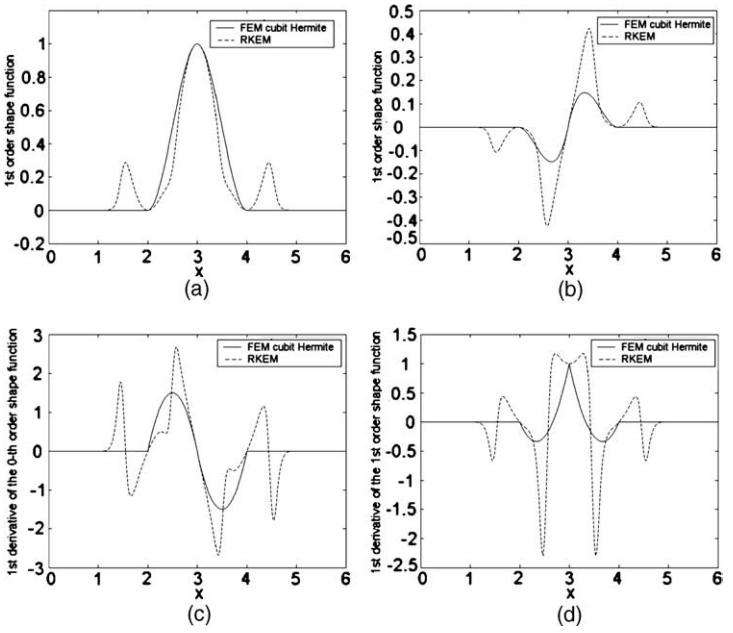

Fig. 8. The global shape functions of 1D $I^1/C^4/P^3$ element: (a) $\Psi_I^{(0)}(\mathbf{x})$, (b) $\Psi_I^{(1)}(\mathbf{x})$, (c) $\mathrm{d}\Psi_I^{(0)}/\mathrm{d}x$, and (d) $\mathrm{d}\Psi_I^{(1)}/\mathrm{d}x$.

where $\boldsymbol{\psi}$ is denoted as the local shape function array and vector $\mathbf{f}$ is the nodal data array, i.e.

$$\boldsymbol{\psi}^{\mathrm{T}} = \left\{\psi_{e,1}^{(00)}, \psi_{e,1}^{(10)}, \psi_{e,1}^{(01)}, \psi_{e,2}^{(00)}, \psi_{e,2}^{(10)}, \psi_{e,2}^{(01)}, \psi_{e,3}^{(00)}, \psi_{e,3}^{(10)}, \psi_{e,3}^{(01)}\psi_{e,4}^{(00)}, \psi_{e,4}^{(10)}, \psi_{e,4}^{(01)}\right\}, \tag{4.187}$$

$$\mathbf{f}^{\mathrm{T}} = \left\{f_{e1}, f_{e1,x}, f_{e1,y}, f_{e2}, f_{e2,x}, f_{e2,y}, f_{e3}, f_{e3,x}, f_{e3,y}, f_{e4}, f_{e4,x}, f_{e4,y}\right\}. \tag{4.188}$$

Based on Przemieniecki [25], we have the explicit expressions for the chosen global partition polynomials,

$$\boldsymbol{\psi}^{\mathrm{T}} = \begin{bmatrix} 1-\xi\eta-(3-2\xi)\xi^2(1-\eta)-(1-\xi)(3-2\eta)\eta^2 \\ (1-\xi)\eta(1-\eta)^2\ell_{ey} \\ -\xi(1-\xi)^2(1-\eta)\ell_{ex} \\ (1-\xi)(3-2\eta)\eta^2+\xi(1-\xi)(1-2\xi)\eta \\ -(1-\xi)(1-\eta)\eta^2\ell_{ey} \\ -\xi(1-\xi)^2\eta\ell_{ex} \\ (3-2\xi)\xi^2\eta-\xi\eta(1-\eta)(1-2\eta) \\ -\xi(1-\eta)\eta^2\ell_{ey} \\ (1-\xi)\xi^2\eta\ell_{ex} \\ (3-2\xi)\xi^2(1-\eta)+\xi\eta(1-\eta)(1-2\eta) \\ \xi\eta(1-\eta)^2\ell_{ey} \\ (1-\xi)\xi^2(1-\eta)\ell_{ex} \end{bmatrix}, \tag{4.189}$$

where $-\infty < \xi, \eta < \infty$.

Assume that the mesh connectivity map is,

$$\Lambda_E \times \Lambda_e \to \Lambda_P : (e_1, i_1)\cdots(e_\ell, i_\ell) \to I.$$

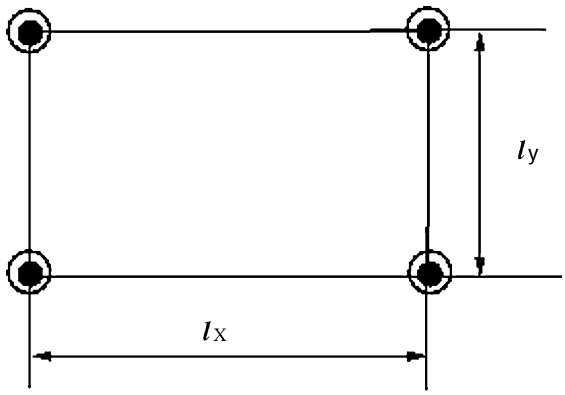

Fig. 9. A globally conforming Gallagher element.

The RKEM global shape function for the rectangular can be expressed as follows:

$$\Psi_I^{(\alpha)}(\mathbf{x}) = \sum_{k=1}^{\ell} \sum_{j \in \Lambda_{e_k}} \left(\mathscr{K}^{\rho}_{e_k,j}(\mathbf{x}) \Delta V_{e_k,j} \right) \psi^{(\alpha)}_{e_k,i_k}(\mathbf{x}). \tag{4.190}$$

4.4. 2D example II: T12P3I(4/3) triangle element

Rectangular element only cannot discretize an arbitrary domain. Here, we propose a two-dimensional globally conforming, bilinear, 12 degrees of freedom triangle element. It is illustrated in Fig. 10. The notation $I^{4/3}$ means that at each nodal point we interpolate the unknown function, say $f(x,y)$, its two first order derivatives, $\partial f/\partial x$ and $\partial f/\partial x$ and its mixed derivative, $\partial^2 f/\partial x \partial y$, which is one-third of the second derivatives. We denote the one-third of second derivative as a cross in Fig. 10. Therefore, in each nodal, there are four degrees of freedom, and there are 12 degrees of freedom in the triangle.

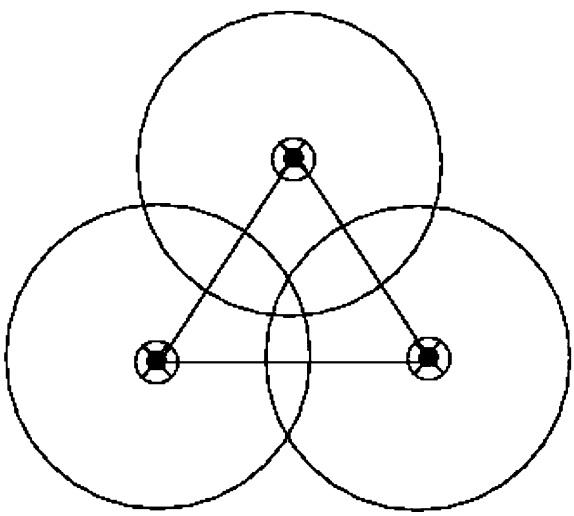

Fig. 10. An bilinear triangle (T12P3I(4/3)) element.

The global partition polynomials in an element can form a local interpolation,

$$\begin{aligned}\mathscr{I}_{\mathrm{loc}}f &= \sum_{i=1}^{3}\left(\psi_{e,i}^{(00)}f_{e,i}+\psi_{e,i}^{(10)}\left.\frac{\partial f}{\partial x}\right|_{(e,i)}+\psi_{e,i}^{(01)}\left.\frac{\partial f}{\partial y}\right|_{(e,i)}+\psi_{e,i}^{(11)}\left.\frac{\partial^2 f}{\partial x\partial y}\right|_{(e,i)}\right)\\ &= c_1+c_2x+c_3y+c_4x^2+c_5xy+c_6y^2+c_7x^3+c_8x^2y+c_9xy^2+c_{10}y^3+c_{11}x^2(x^2+xy+y^2)\\ &\quad +c_{12}y^2(x^2+xy+y^2).\end{aligned} \tag{4.191}$$

To link the nodal data with constants, c's, we define vectors, $\boldsymbol{\psi}$, $\mathbf{f}$, $\mathbf{p}$, and $\mathbf{c}$:

$$\boldsymbol{\psi}_e^{\mathrm{T}}(\mathbf{x}) := \{\psi_{e,1}^{(00)},\psi_{e,1}^{(10)},\psi_{e,1}^{(01)},\psi_{e,1}^{(11)},\psi_{e,2}^{(00)},\psi_{e,2}^{(10)},\psi_{e,2}^{(01)},\psi_{e,2}^{(11)},\psi_{e,3}^{(00)},\psi_{e,3}^{(10)},\psi_{e,3}^{(01)},\psi_{e,3}^{(11)}\}, \tag{4.192}$$

$$\mathbf{f}_e^{\mathrm{T}} := \{f_1,f_{1x},f_{1y},f_{1xy},f_2,f_{2x},f_{2y},f_{2xy},f_3,f_{3x},f_{3y},f_{3xy}\}_e, \tag{4.193}$$

$$\mathbf{p}^{\mathrm{T}}(\mathbf{x}) := \{1,x,y,x^2,xy,y^2,x^3,x^2y,xy^2,y^3,x^2(x^2+xy+y^2),y^2(x^2+xy+y^2)\}, \tag{4.194}$$

$$\mathbf{c}_e^{\mathrm{T}} := \{c_1,c_2,c_3,c_4,c_5,c_6,c_7,c_8,c_9,c_{10},c_{11},c_{12}\}_e. \tag{4.195}$$

We can write that

$$\mathscr{I}_{\mathrm{loc}}f = \boldsymbol{\psi}_e^{\mathrm{T}}\mathbf{f}_e = \mathbf{p}^{\mathrm{T}}\mathbf{c}_e. \tag{4.196}$$

The nodal values are related with coefficients c's by a set of 12 simultaneous linear algebraic equations

$$\mathbf{f}_e = \mathbf{C}_e\mathbf{c}_e, \tag{4.197}$$

where matrix $\mathbf{C}_e$ is defined by Eq. (4.198).

$$\mathbf{C}_e = \begin{vmatrix}
1 & x_1 & y_1 & x_1^2 & x_1y_1 & y_1^2 & x_1^3 & x_1^2y_1 & x_1y_1^2 & y_1^3 & x_1^2(x_1^2+x_1y_1+y_1^2) & y_1^2(x_1^2+x_1y_1+y_1^2)\\
0 & 1 & 0 & 2x_1 & y_1 & 0 & 3x_1^2 & 2x_1y_1 & y_1^2 & 0 & x_1(4x_1^2+3x_1y_1+2y_1^2) & y_1^2(2x_1+y_1)\\
0 & 0 & 1 & 0 & x_1 & 2y_1 & 0 & x_1^2 & 2x_1y_1 & 3y_1^2 & x_1^2(x_1+2y_1) & y_1(4y_1^2+3x_1y_1+2x_1^2)\\
0 & 0 & 0 & 0 & 1 & 0 & 0 & 2x_1 & 2y_1 & 0 & 3x_1^2+4x_1y_1 & 3y_1^2+4x_1y_1\\
1 & x_2 & y_2 & x_2^2 & x_2y_2 & y_2^2 & x_2^3 & x_2^2y_2 & x_2y_2^2 & y_2^3 & x_2^2(x_2^2+x_2y_2+y_2^2) & y_2^2(x_2^2+x_2y_2+y_2^2)\\
0 & 1 & 0 & 2x_2 & y_2 & 0 & 3x_2^2 & 2x_2y_2 & y_2^2 & 0 & x_2(4x_2^2+3x_2y_2+2y_2^2) & y_2^2(2x_2+y_2)\\
0 & 0 & 1 & 0 & x_2 & 2y_2 & 0 & x_2^2 & 2x_2y_2 & 3y_2^2 & x_2^2(x_2+2y_2) & y_2(4y_2^2+3x_2y_2+2x_2^2)\\
0 & 0 & 0 & 0 & 1 & 0 & 0 & 2x_2 & 2y_2 & 0 & 3x_2^2+4x_2y_2 & 3y_2^2+4x_2y_2\\
1 & x_3 & y_3 & x_3^2 & x_3y_3 & y_3^2 & x_3^3 & x_3^2y_3 & x_3y_3^2 & y_3^3 & x_3^2(x_3^2+x_3y_3+y_3^2) & y_3^2(x_3^2+x_3y_3+y_3^2)\\
0 & 1 & 0 & 2x_3 & y_3 & 0 & 3x_3^2 & 2x_3y_3 & y_3^2 & 0 & x_3(4x_3^2+3x_3y_3+2y_3^2) & y_3^2(2x_3+y_3)\\
0 & 0 & 1 & 0 & x_3 & 2y_3 & 0 & x_3^2 & 2x_3y_3 & 3y_3^2 & x_3^2(x_3+2y_3) & y_3(4y_3^2+3x_3y_3+2x_3^2)\\
0 & 0 & 0 & 0 & 1 & 0 & 0 & 2x_3 & 2y_3 & 0 & 3x_3^2+4x_3y_3 & 3y_3^2+4x_3y_3
\end{vmatrix}. \tag{4.198}$$

One can then find vector $\mathbf{c}_e$ by solving the linear algebraic equation,

$$\mathbf{c}_e = \mathbf{C}_e^{-1}\mathbf{f}. \tag{4.199}$$

Then, the global partition polynomials can be found as

$$\boldsymbol{\psi}_e(\mathbf{x}) = \mathbf{C}_e^{-\mathrm{T}}\mathbf{p}(\mathbf{x}). \tag{4.200}$$

Assume that the mesh connectivity map is as usual

$$\Lambda_E\times\Lambda_e\to\Lambda_P : (e_1,i_1)\cdots(e_\ell,i_\ell)\to I. \tag{4.201}$$

The RKEM global shape functions of the triangle resume the same formula (Fig. 11),

$$\Psi_I^{(\alpha)}(\mathbf{x}) = \sum_{k=1}^{\ell} \sum_{j \in \Lambda_{e_k}} (\mathscr{K}^{\rho}_{e_k,j}(\mathbf{x}) \Delta V_{e_k,j}) \psi^{(\alpha)}_{e_k,ik}(\mathbf{x}). \tag{4.202}$$

4.5. 2D example III: Q12P3I1 quadrilateral element

One can consider constructing quadrilateral element by using the same technique (Fig. 12). The element interpolation provided by the global partition polynomials in an element is

$$\begin{aligned} \mathscr{I}_{\text{loc}} f &= \sum_{i=1}^{4} \left(\psi^{(00)}_{e,i} f_{e,i} + \psi^{(10)}_{e,i} \left.\frac{\partial f}{\partial x}\right|_{(e,i)} + \psi^{(01)}_{e,i} \left.\frac{\partial f}{\partial y}\right|_{(e,i)} \right) \\ &= c_1 + c_2 x + c_3 y + c_4 x^2 + c_5 xy + c_6 y^2 + c_7 x^3 + c_8 x^2 y + c_9 xy^2 + c_{10} y^3 + c_{11} x^2 (x^2 + xy + y^2) \\ &\quad + c_{12} y^2 (x^2 + xy + y^2). \end{aligned} \tag{4.203}$$

To link the nodal data with constants, c's, vectors, $\boldsymbol{\psi}$, $\mathbf{f}$, $\mathbf{p}$, and $\mathbf{c}$ are defined

$$\boldsymbol{\psi}_e^{\mathrm{T}}(\mathbf{x}) := \left\{ \psi^{(00)}_{e,1}, \psi^{(10)}_{e,1}, \psi^{(01)}_{e,1}, \psi^{(00)}_{e,2}, \psi^{(10)}_{e,2}, \psi^{(01)}_{e,2}, \psi^{(00)}_{e,3}, \psi^{(10)}_{e,3}, \psi^{(01)}_{e,3}, \psi^{(00)}_{e,4}, \psi^{(10)}_{e,4}, \psi^{(01)}_{e,4} \right\}, \tag{4.204}$$

$$\mathbf{f}_e^{\mathrm{T}} := \{ f_1, f_{1x}, f_{1y}, f_2, f_{2x}, f_{2y}, f_3, f_{3x}, f_{3y}, f_4, f_{4x}, f_{4y} \}_e, \tag{4.205}$$

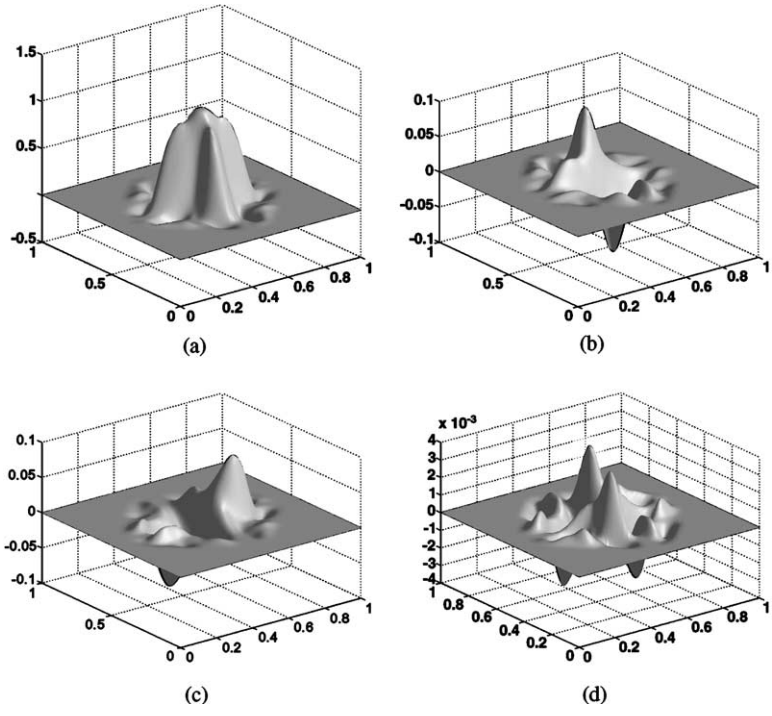

Fig. 11. The four global shape functions of T12P3I(4/3) element: (a) $\Psi_I^{(00)}(\mathbf{x})$, (b) $\Psi_I^{(10)}(\mathbf{x})$, (c) $\Psi_I^{(01)}(\mathbf{x})$, and (d) $\Psi_I^{(11)}(\mathbf{x})$.

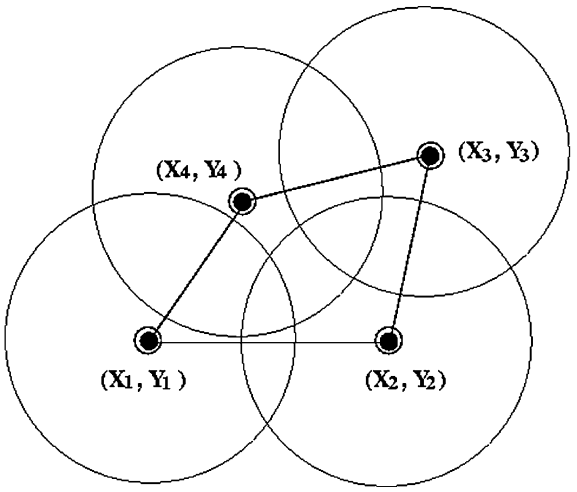

Fig. 12. Illustration of Q12P3I1 quadrilateral element.

$$\mathbf{p}^{\mathrm{T}}(\mathbf{x}) := \{1, x, y, x^2, xy, y^2, x^3, x^2y, xy^2, y^3, x^2(x^2+xy+y^2), y^2(x^2+xy+y^2)\}, \tag{4.206}$$

$$\mathbf{c}_e^{\mathrm{T}} := \{c_1, c_2, c_3, c_4, c_5, c_6, c_7, c_8, c_9, c_{10}, c_{11}, c_{12}\}_e. \tag{4.207}$$

We can write that

$$\mathscr{I}_{\mathrm{loc}} f = \boldsymbol{\psi}_e^{\mathrm{T}} \mathbf{f}_e = \mathbf{p}^{\mathrm{T}} \mathbf{c}_e. \tag{4.208}$$

Again, the nodal values are related with coefficients c's by a system of 12 linear algebraic equations

$$\mathbf{f}_e = \mathbf{C}_e \mathbf{c}_e, \tag{4.209}$$

where matrix $\mathbf{C}_e$ is defined by Eq. (4.210). By solving the linear algebraic equation, one can

$$\mathbf{C}_e = \begin{vmatrix}
1 & x_1 & y_1 & x_1^2 & x_1y_1 & y_1^2 & x_1^3 & x_1^2y_1 & x_1y_1^2 & y_1^3 & x_1^2(x_1^2+x_1y_1+y_1^2) & y_1^2(x_1^2+x_1y_1+y_1^2) \\
0 & 1 & 0 & 2x_1 & y_1 & 0 & 3x_1^2 & 2x_1y_1 & y_1^2 & 0 & x_1(4x_1^2+3x_1y_1+2y_1^2) & y_1^2(2x_1+y_1) \\
0 & 0 & 1 & 0 & x_1 & 2y_1 & 0 & x_1^2 & 2x_1y_1 & 3y_1^2 & x_1^2(x_1+2y_1) & y_1(4y_1^2+3x_1y_1+2x_1^2) \\
1 & x_2 & y_2 & x_2^2 & x_2y_2 & y_2^2 & x_2^3 & x_2^2y_2 & x_2y_2^2 & y_2^3 & x_2^2(x_2^2+x_2y_2+y_2^2) & y_2^2(x_2^2+x_2y_2+y_2^2) \\
0 & 1 & 0 & 2x_2 & y_2 & 0 & 3x_2^2 & 2x_2y_2 & y_2^2 & 0 & x_2(4x_2^2+3x_2y_2+2y_2^2) & y_2^2(2x_2+y_2) \\
0 & 0 & 1 & 0 & x_2 & 2y_2 & 0 & x_2^2 & 2x_2y_2 & 3y_2^2 & x_2^2(x_2+2y_2) & y_2(4y_2^2+3x_2y_2+2x_2^2) \\
1 & x_3 & y_3 & x_3^2 & x_3y_3 & y_3^2 & x_3^3 & x_3^2y_3 & x_3y_3^2 & y_3^3 & x_3^2(x_3^2+x_3y_3+y_3^2) & y_3^2(x_3^2+x_3y_3+y_3^2) \\
0 & 1 & 0 & 2x_3 & y_3 & 0 & 3x_3^2 & 2x_3y_3 & y_3^2 & 0 & x_3(4x_3^2+3x_3y_3+2y_3^2) & y_3^2(2x_3+y_3) \\
0 & 0 & 1 & 0 & x_3 & 2y_3 & 0 & x_3^2 & 2x_3y_3 & 3y_3^2 & x_3^2(x_3+2y_3) & y_3(4y_3^2+3x_3y_3+2x_3^2) \\
1 & x_4 & y_4 & x_4^2 & x_4y_4 & y_4^2 & x_4^3 & x_4^2y_4 & x_4y_4^2 & y_4^3 & x_4^2(x_4^2+x_4y_4+y_4^2) & y_4^2(x_4^2+x_4y_4+y_4^2) \\
0 & 1 & 0 & 2x_4 & y_4 & 0 & 3x_3^2 & 2x_3y_3 & y_4^2 & 0 & x_4(4x_4^2+3x_4y_4+2y_4^2) & y_4^2(2x_4+y_4) \\
0 & 0 & 1 & 0 & x_4 & 2y_4 & 0 & x_4^2 & 2x_4y_4 & 3y_4^2 & x_4^2(x_4+2y_4) & y_4(4y_4^2+3x_4y_4+2x_4^2)
\end{vmatrix} \tag{4.210}$$

then find vector $\mathbf{c}_e$

$$\mathbf{c}_e = \mathbf{C}_e^{-1} \mathbf{f} \tag{4.211}$$

and then the global partition polynomials

$$\boldsymbol{\psi}_e(\mathbf{x}) = \mathbf{C}_e^{-\mathrm{T}}\mathbf{p}(\mathbf{x}). \tag{4.212}$$

5. Numerical examples

To validate the method, the proposed RKEM interpolants are tested for their interpolation error and convergence rate in Galerkin procedure. Systematic numerical experiments will be reported in Parts III and IV of this work [24,26]. Here two examples are presented to give a flavor of this class of globally conforming interpolants.

We first examined the interpolation error of both Q12P1I1 and Q16P2I2 quadrilateral RKEM Hermite interpolants in a two-dimensional domain (Fig. 13). Consider the following trigonometric function,

$$w(x,y) = C\sin\left(\frac{x}{2.0}\right)\sin\left(\frac{y}{1.0}\right), \quad 0 \leqslant x \leqslant 2.0 \text{ and } 0.0 \leqslant y \leqslant 1.0,$$

where $C = 1.0/418$.

We have used both Q12P1I1 and Q16P2I2 quadrilateral elements and their shape functions to interpolate the given function in three different meshes: 21×21, 41×41, and 81×81.

First of all, as the numerical results indicated, this is a multi-dimensional compatible interpolation scheme, and one gets smoothed derivatives up to second order. The interpolation errors for both interpolants are 2.0 and 3.2 in L^2 norm and 1.0 and 2.1 in H^1 norm, which are what we expected. The similar interpolation error estimate holds when we change the position of some interior nodes to render a general quadrilateral 2D mesh. Therefore, the 2D interpolation test shows that we have successfully constructed a minimum, global conforming Hermite hierarchy in multi-dimensions.

In the second example, we use T12P3I(4/3) triangle element to calculate the deformation of a simply supported equilateral triangle thin plate, which is subjected a uniformly load.

The problem statement is:

$$\nabla^2\nabla^2 w = \frac{p}{D} \quad \forall(x,y) \in \Omega, \tag{5.213}$$

$$w = 0 \quad \forall(x,y) \in \partial\Omega, \tag{5.214}$$

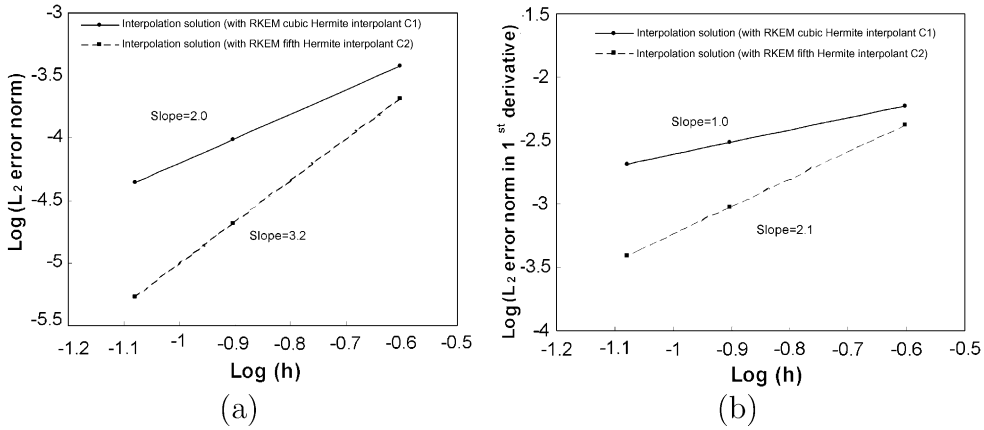

Fig. 13. Interpolation error for both Q12P1I1 and Q16P2I2 RKEM Hermite interpolants in a rectangular domain: (a) L^2 norm and (b) H^1 norm.

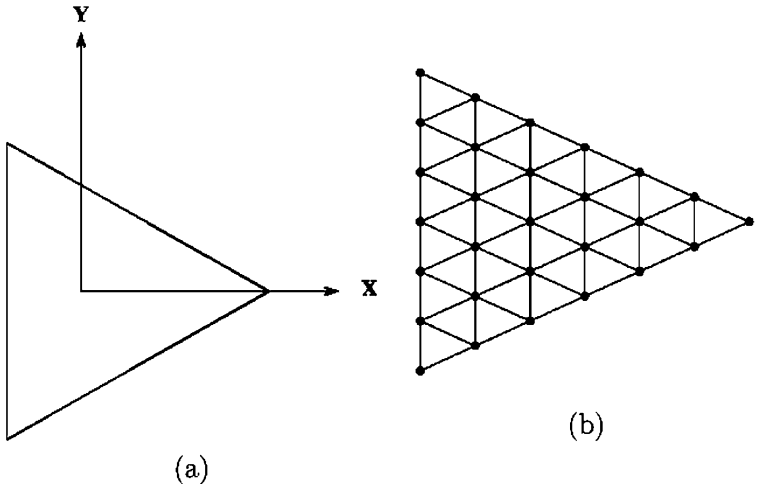

Fig. 14. Problem domain and mesh for simply supported triangular plate: (a) problem domain and (b) 36 node.

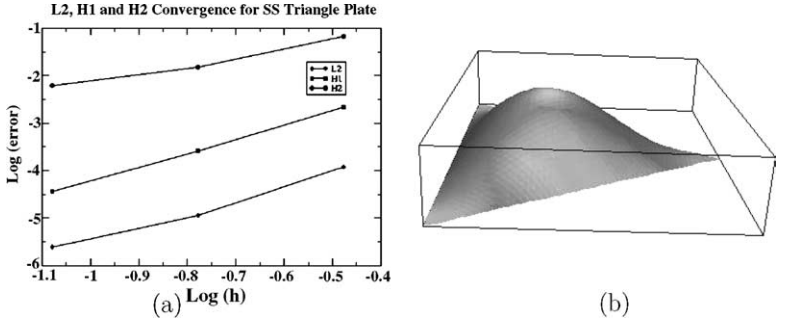

Fig. 15. Numerical example II: (a) convergence results and (b) deformed shape for an equilateral thin plate.

$$\frac{\partial w}{\partial s} = 0 \quad \forall (x, y) \in \partial\Omega, \tag{5.215}$$

$$M_n = -D\left(\frac{\partial^2 w}{\partial n^2} + v\frac{\partial^2 w}{\partial s^2}\right) = 0 \quad \forall (x, y) \in \partial\Omega, \tag{5.216}$$

where direction n is normal to the edge of the thin plate and the direction s is tangential to the edge of the thin plate.

The problem domain and triangle discretization are illustrated in Fig. 14. The computed deformed shape and convergence results are displayed in Fig. 15. A detailed discussion on this problem can be found in both Parts III and IV of this work [24,26].

6. Closure

This is the second paper in a series devoted to a new class of partition of unities, collectively called RKEM. In the development of RKEM, we remove the limitations on both smoothness and high order

Kronecker delta properties of the finite element method, while at the same time, we maintain the polynomial reproducing property and function interpolation property. Unlike most meshfree interpolants, RKEM interpolant do not need special treatment to enforce Dirichlet boundary conditions. Preliminary results show satisfactory performance of the new method in solving boundary value problems of higher order differential equations over domains of any dimension, and of arbitrary boundary conditions. Detailed numerical computations shall be reported in subsequent papers.

This new method also eliminates a major weakness of meshfree interpolants, which lose optimal convergence rate while enforcing Dirichlet boundary conditions when the problem is posed over a multiple dimensional domain and when the polynomial reproducing order is larger than one. It should be noted that in constructing of multiple dimensional RKEM shape functions we have systematically used nodal integration technique to form the meshfree part of the interpolant.

In conclusion, unlike traditional FEM shape functions, RKEM interpolants can be used directly in a prime variational formulation in solving a high order differential equation, and unlike most meshfree interpolants, RKEM interpolant can satisfy Dirichlet boundary conditions without ant difficulties.

In the end, we would like to point out that the basic strategy or philosophy of RKEM method is to build the interpolation field on a special partition of unity, which we call as *global partition polynomials*. In order to recover the Kronecker delta property, we use the RKPM meshfree interpolant to localize the global partition polynomials such that the global RKEM basis function is a truly interpolant, which satisfies the general higher order Kronecker delta properties. By doing so, the smoothness of an interpolant is dictated by the window function of the meshfree kernel function, which can be controlled by the user arbitrarily.

Acknowledgements

This work is made possible by the support from NSF under grants CMS-0239130 to University of California (Berkeley), DMI-0115079 to Northwestern University, and DMS-0106781 to University of Iowa, which are greatly appreciated.

References

[1] J.H. Argyris, I. Fried, D.W. Scharpf, The TUBA family of plate elements for the matrix displacement method, Aeronaut. Roy. Aeronaut. Soc. 72 (1968) 701–709.
[2] R.E. Barnhill, G. Birkhoff, W.J. Gordon, Smooth interpolation in triangles, J. Approx. Theory 8 (1973) 114–128.
[3] G.P. Bazeley, Y.K. Cheung, B.M. Irons, O.C. Zienkiewicz, Triangle elements in bending: conforming and nonconforming solutions, in: Proc. 1st Conference on Matrix Methods in Structural Mechanics, Wright-Patterson, AFB, OH, 1965.
[4] K. Bell, A refined triangular plate bending finite element, Int. J. Numer. Methods Engrg. 1 (1969) 101–122.
[5] G. Birkhoff, M.H. Schultz, R.S. Varga, Piecewise Hermite interpolation in one and two variables with applications to partial differential equations, Numer. Math. 11 (1968) 232–256.
[6] F.K. Bogner, R.L. Fox, L.A. Schmit, The generation of inter-element compatible stiffness and mass matrices by the use of interpolation formulae, in: Proc. 1st Conference on Matrix Methods in Structural Mechanics, Wright-Patterson, AFB, OH.
[7] R.W. Clough, J. Tocher, Finite element stiffness matrices for the analysis of plate bending, in: Proc. 1st Conference on Matrix Methods in Structural Mechanics, Wright-Patterson, AFB, OH, 1965.
[8] F.B. de Veubeke, Bending and stretching of plates—special models for upper and lower bounds, in: Proc. 1st Conference on Matrix Methods in Structural Mechanics, Wright-Patterson, AFB, OH, 1965.
[9] F.B. de Veubeke, A conforming finite element for plate bending, Int. J. Solids Struct. 4 (1968) 95–108.
[10] C. Felippa, R.W. Clough, The finite element in solid mechanics, in: SIAM-AMS Proceedings, vol. 2, American Mathematical Society, Providence, RI, 1970, pp. 210–252.
[11] R.H. Gallagher, R.A. Cellatly, J. Padlog, R.H. Mallett, A discrete element procedure for thin-shell instability analysis, AIAA J. 5 (1967) 138–145.

[12] W. Han, X. Meng, Error analysis of the reproducing kernel particle method, Comput. Methods Appl. Mech. Engrg. 190 (2001) 6157–6181.
[13] S. Hao, H.S. Park, W.K. Liu, Moving particle finite element method, Int. J. Numer. Methods Engrg. 53 (2002) 1937–1958.
[14] T.J.R. Hughes, The Finite Element Method, Prentice Hall, Englewood Cliffs, NJ, 1987.
[15] B.M. Irons, A Conforming quadratic triangular element for plate bending, Int. J. Numer. Methods Engrg. 1 (1969) 29–45.
[16] B.M. Irons, A. Razzaque, Experience with the patch test for convergence of finite element methods, in: A.K. Aziz (Ed.), Mathematical Foundations of Finite Element Method with Applications to Partial Differential Equations, Academic Press, 1972, pp. 557–587.
[17] S. Li, W.K. Liu, Meshfree and particle methods and their applications, Appl. Mech. Rev. 55 (2002) 1–34.
[18] W.K. Liu, Y. Chen, R.A. Uras, T.C. Chang, Generalized multiple scale reproducing kernel particle methods, Comput. Methods Appl. Mech. Engrg. 139 (1996) 91–157.
[19] W.K. Liu, R.A. Uras, Y. Chen, Enrichment of the finite element method with the reproducing kernel particle method, J. Appl. Mech. 64 (1997) 861–870.
[20] W.K. Liu, W. Han, H. Lu, S. Li, J. Cao, Reproducing kernel element method: Part I. Theoretical formulation, Comput. Methods Appl. Mech. Engrg., in this issue.
[21] W.K. Liu, S. Jun, S. Li, J. Adee, T. Belytschko, Reproducing kernel particle methods for structural dynamics, Int. J. Numer. Methods Engrg. 38 (1995) 1655–1679.
[22] W.K. Liu, S. Jun, Y.F. Zhang, Reproducing kernel particle methods, Int. J. Numer. Methods Fluids 20 (1995) 1081–1106.
[23] W.K. Liu, S. Li, T. Belytschko, Moving least square reproducing kernel method part I: methodology and convergence, Comput. Methods Appl. Mech. Engrg. 143 (1997) 422–453.
[24] H. Lu, S. Li, D.C. Simkins Jr., W.K. Liu, J. Cao, Reproducing kernel element method Part III. Generalized enrichment and applications, Comput. Methods Appl. Mech. Engrg., in this issue.
[25] J.S. Przemieniecki, Theory of Matrix Structural Analysis, McGraw-Hill, 1968.
[26] D.C. Simkins Jr., S. Li, H. Lu, W.K. Liu, Reproducing kernel element method. Part IV. Globally compatible C^n $(n \geqslant 1)$ triangle hierarchy, Comput. Methods Appl. Mech. Engrg., in this issue.
[27] J.H. Bramble, M. Zlamal, Triangle elements in the finite element method, Mathematics of Computation 24 (1970) 809–820.
[28] G. Birkhoff, W.J. Gordon, The draftsman's and related equations, J. Approx. Theory 1 (1986) 199–208.
[29] G. Birkhoff, Interpolation to boundary data in triangles, J. Mathematical Anal. Applic. 42 (1973) 474–484.